

Level crossings, excess times and transient plasma–wall interactions in fusion plasmas: Theoretical predictions and simulations

A. Theodorsen^{1, a)} and O. E. Garcia^{1, b)}

*Department of Physics and Technology, UiT The Arctic University of Norway,
N-9037 Tromsø, Norway*

(Dated: 20 May 2019)

Based on a stochastic model for intermittent fluctuations in the boundary region of magnetically confined plasmas, an expression for the level crossing rate is derived from the joint distribution of the process and its derivative. From this the average time spent by the process above a certain threshold level is obtained, and limits of both high and low intermittency are investigated and compared to previously known results. In the case of a highly intermittent process, the distribution of time spent above threshold is obtained. This expression is verified numerically, and the distribution of time above threshold is explored for other intermittency regimes. The numerical results compare favorably to known results for the distribution of time above the mean threshold for an Ornstein-Uhlenbeck process. This contribution generalizes the excess time statistics for the stochastic model and provides novel predictions of plasma–wall interactions due to transient transport events associated with radial motion of blob-like structures in the scrape-off layer.

^{a)}Electronic mail: audun.theodorsen@uit.no

^{b)}Electronic mail: odd.erik.garcia@uit.no

I. INTRODUCTION

Plasma–wall interactions remain an outstanding challenge in the quest for controlled thermonuclear fusion based on magnetic confinement.^{1–3} Transient transport events due to filamentary structures moving through the scrape-off layer may cause detrimental sputtering and erosion of the main chamber walls. The interaction between the hot plasma and material surfaces depends on the turbulence-induced particle and heat fluxes, so gaining insight into the statistical properties of plasma fluctuations in the boundary region is of considerable interest.

The radial propagation of blob-like structures results in large-amplitude bursts in single-point measurements in the scrape-off layer. Recent analysis of such measurement time series using conditional averaging have elucidated the statistical properties of large-amplitude fluctuations.^{4–10} The experimental results provide evidence that plasma fluctuations can be described as a super-position of uncorrelated pulses with fixed, exponential pulse shape of constant duration and exponentially distributed pulse amplitudes. These are the basic assumptions behind a recently suggested stochastic model for intermittent plasma fluctuations in the scrape-off layer region.^{6–15} This model describes many experimental findings from the boundary region of magnetized plasmas, including bursty fluctuations, skewed and flattened probability density functions (PDFs) and accordingly a parabolic relation between the skewness and flatness moments for a broad range of parameters.^{4–10,16,17}

The stochastic model can be extended in several ways, including adding a noise term,¹⁸ using different pulse shapes^{17,19–21} or allowing for a distribution of pulse durations.^{20,21} In this contribution, which is an extended version of Ref. 15, the joint distribution function of the process and its derivative is derived. This is shown to give novel predictions of the intermittent features of plasma fluctuations, in particular the rate of level crossings and excess time statistics, that is, the duration of time intervals where the signal exceeds some prescribed threshold level.^{22–26} Although of particular interest for plasma–wall interactions in fusion grade plasmas, the stochastic model is prototypical for many intermittent systems, and the results find applications in a broad range of fields (see for example Ref. 26 and references therein).

The rate of level crossings has also been investigated in many different settings.^{27–34} The normal limit for level crossings and average time above threshold have previously been compared with measurement data from a basic laboratory experiment and rocket data from the polar ionosphere, and the discrepancy interpreted as a signature of intermittency in the underlying processes.^{24,25}

Given the joint PDF $P_{\Phi\dot{\Phi}}(\Phi, \dot{\Phi})$ for a stationary random variable $\Phi(t)$ and its derivative $\dot{\Phi} =$

$d\Phi/dt$, the number of up-crossings of the level Φ in a time interval of duration T is given by integrating over all positive values of the derivative^{22–25},

$$X(\Phi) = T \int_0^\infty d\dot{\Phi} \dot{\Phi} P_{\Phi\dot{\Phi}}(\Phi, \dot{\Phi}). \quad (1)$$

For independent, normally distributed $\Phi(t)$ and $\dot{\Phi}$, this gives the celebrated result known as the Rice formula,^{22–26}

$$X(\Phi) = T \frac{\dot{\Phi}_{\text{rms}}}{2\pi\Phi_{\text{rms}}} \exp\left(-\frac{(\Phi - \langle\Phi\rangle)^2}{2\Phi_{\text{rms}}^2}\right), \quad (2)$$

where $\langle\Phi\rangle$ is the mean value of Φ and Φ_{rms} and $\dot{\Phi}_{\text{rms}}$ are the standard deviation or root mean square (rms) values of Φ and $\dot{\Phi}$, respectively. The rate of level crossings is clearly largest for threshold values close to the mean value of Φ . In this contribution, we will frequently use the normalization

$$\tilde{\Phi} = \frac{\Phi - \langle\Phi\rangle}{\Phi_{\text{rms}}}, \quad (3)$$

giving

$$X(\tilde{\Phi}) = T \frac{\dot{\Phi}_{\text{rms}}}{2\pi\Phi_{\text{rms}}} \exp\left(-\frac{\tilde{\Phi}^2}{2}\right). \quad (4)$$

The average time $\langle\Delta T\rangle$ spent above a threshold value Φ by the stationary process is given by the ratio of the total time spent above the level Φ and the number of up-crossings X in an interval of duration T . The former is by definition given by the complementary cumulative distribution function $1 - C_\Phi$ for the process, where $C_\Phi(\Phi)$ is the cumulative distribution function. This gives the average excess time as

$$\langle\Delta T\rangle(\Phi) = T \frac{1 - C_\Phi(\Phi)}{X(\Phi)}. \quad (5)$$

For jointly normally distributed Φ and $\dot{\Phi}$ with zero correlation (that is, the processes are independent), the average excess time is given by^{23–25}

$$\langle\Delta T\rangle(\tilde{\Phi}) = \pi \frac{\Phi_{\text{rms}}}{\dot{\Phi}_{\text{rms}}} \text{erfc}\left(\frac{\tilde{\Phi}}{\sqrt{2}}\right) \exp\left(\frac{\tilde{\Phi}^2}{2}\right), \quad (6)$$

where erfc denotes the complementary error function.

The goal of this contribution is to derive expressions for level crossings and excess times for the filtered Poisson process, also called the shot-noise model. In Sec. II, the filtered Poisson process with a double exponential pulse shape with fixed pulse duration time and exponentially distributed amplitudes is introduced, and some of its statistical properties are reviewed. The derivative of the

process is discussed, and the joint PDF between the process and its derivative is found. In Sec. III, expressions for the rate of level crossings and the average excess time for the FPP are given. Limits of the one-sided waveform, the normal limit and the limit of strong intermittency are discussed. Finally, the rate of level crossings for a filtered Poisson process with Laplace distributed amplitudes is considered and compared to the exponential case. In Sec. IV, we discuss the distribution of excess times in the strong intermittency limit and in the normal limit. Sec. V gives numerical results for the distribution of excess times in the general case, and compares this to the analytic expressions from Sec. IV. The convergence of the rate of level crossings to its analytic expression is also considered. Concluding remarks are given in Sec. VI.

II. THE FILTERED POISSON PROCESS

In this section, the filtered Poisson process is introduced and its general features are discussed.

A. Superposition of pulses

The process can be described as a super-position of uncorrelated pulses,^{6–15,19,35–37}

$$\Phi_K(t) = \sum_{k=1}^{K(T)} A_k \varphi\left(\frac{t - t_k}{\tau_d}\right), \quad (7)$$

where t_k is the pulse arrival time for event k , A_k is the pulse amplitude and the pulse shape $\varphi(s)$ is assumed to be the same for all events. In Eq. (7) the sum is over exactly K pulses present in a record of duration T , and the pulse arrival times are assumed to have a uniform distribution. From this it follows that the number of pulses $K(T)$ is Poisson distributed with constant rate $1/\tau_w$,

$$P_K(K) = \frac{1}{K!} \left(\frac{T}{\tau_w}\right)^K \exp\left(-\frac{T}{\tau_w}\right). \quad (8)$$

Thus, the waiting time between pulses are exponentially distributed with mean value τ_w .

In the following, the pulse shape is described by a two-sided exponential function

$$\varphi(s) = \begin{cases} \exp(s/\lambda), & s < 0, \\ \exp(-s/(1-\lambda)), & s \geq 0, \end{cases} \quad (9)$$

where s is a unitless variable, τ_d is the pulse duration and λ is a pulse shape asymmetry parameter restricted to the range $0 < \lambda < 1$. The ratio between the pulse duration and average waiting time,

$$\gamma = \frac{\tau_d}{\tau_w}, \quad (10)$$

determines the degree of pulse overlap and is the most fundamental parameter of the stochastic model.

Assuming the PDF of A is an exponential distribution,

$$P_A(A) = \frac{1}{\langle A \rangle} \exp \left(-\frac{A}{\langle A \rangle} \right), \quad A > 0, \quad (11)$$

the stationary distribution of the random variable $\Phi(t)$ can be shown to be a Gamma distribution with shape parameter γ and scale parameter $\langle A \rangle$;^{12,13,21,32,38}

$$P_\Phi(\Phi) = \frac{1}{\langle A \rangle \Gamma(\gamma)} \left(\frac{\Phi}{\langle A \rangle} \right)^{\gamma-1} \exp \left(-\frac{\Phi}{\langle A \rangle} \right). \quad (12)$$

where $\Gamma(x)$ is the gamma function with variable x , given in Ref. 39, Eq. 5.2.1. The complementary CDF of Φ is then given by

$$1 - C_\Phi(\Phi) = Q(\gamma, \gamma\Phi / \langle \Phi \rangle), \quad (13)$$

where $Q(s, x)$ is the regularized upper incomplete gamma function with parameter s and variable x , given in Ref. 39, Eq. 8.2.4. In this contribution, we will also use the upper incomplete gamma function $\Gamma(s, x)$, given in Ref. 39, Eq. 8.2.2.

The complementary cumulative distribution function as a function of the threshold level for various values of γ is presented in Fig. 1. As γ increases, this function approaches that of a normal distribution and, in the normal regime $\gamma \gg 1$, the fraction of time above threshold falls rapidly with increasing threshold level since the fluctuations in the signal are concentrated around the mean value. In the strong intermittency regime, $\gamma \ll 1$, the signal spends long periods of time close to zero value as few pulses overlap significantly. Thus, the total time above threshold increases rapidly as the threshold approaches zero.

Correspondingly, the characteristic function of Φ is

$$\langle \exp(i\Phi u) \rangle = (1 - i \langle A \rangle u)^{-\gamma}. \quad (14)$$

It can likewise be shown that the cumulants of the process are given by^{12,13}

$$\kappa_n = \gamma \langle A^n \rangle I_n, \quad (15)$$

where

$$I_n = \int_{-\infty}^{\infty} ds [\varphi(s)]^n. \quad (16)$$

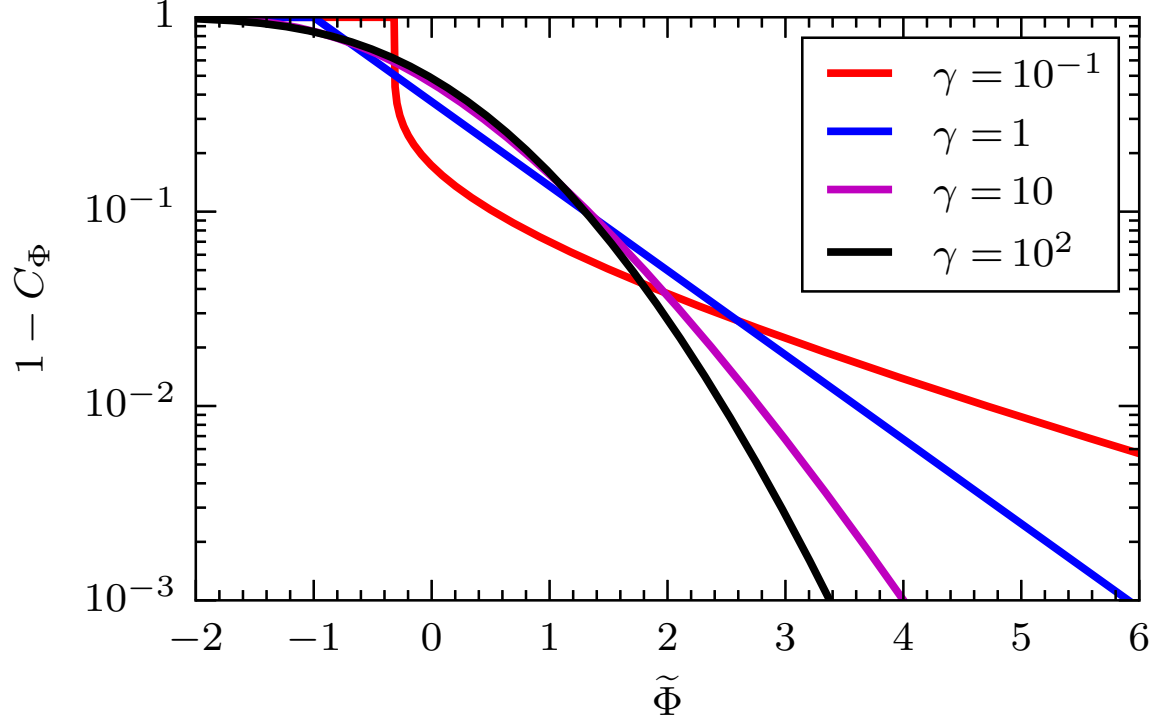


FIG. 1: The complementary cumulative distribution function of the stochastic process for various values of γ .

With the pulse shape given in Eq. (9), $I_n = 1/n$ and using that for exponentially distributed variables, we have $\langle A^n \rangle = n! \langle A \rangle^n$, we have that the cumulants for Φ are

$$\kappa_n = (n-1)! \gamma \langle A \rangle^n. \quad (17)$$

Note that the cumulants, and therefore also the PDF, are independent of λ . Given the cumulants, we can find the lowest order moments of the process:

$$\langle \Phi \rangle = \gamma \langle A \rangle, \quad (18a)$$

$$\Phi_{\text{rms}}^2 = \gamma \langle A \rangle^2, \quad (18b)$$

$$S_\Phi = \frac{2}{\gamma^{1/2}}, \quad (18c)$$

$$F_\Phi = 3 + \frac{6}{\gamma}. \quad (18d)$$

Here, S_Φ is the skewness of the random variable Φ and F_Φ is its flatness. The relative fluctuation level is $\Phi_{\text{rms}} / \langle \Phi \rangle = 1/\gamma^{1/2}$. There is a parabolic relation between skewness and flatness: $F_\Phi(S_\Phi) = 3 + 3S_\Phi^2/2$. It can be shown that the distribution of the normalized process

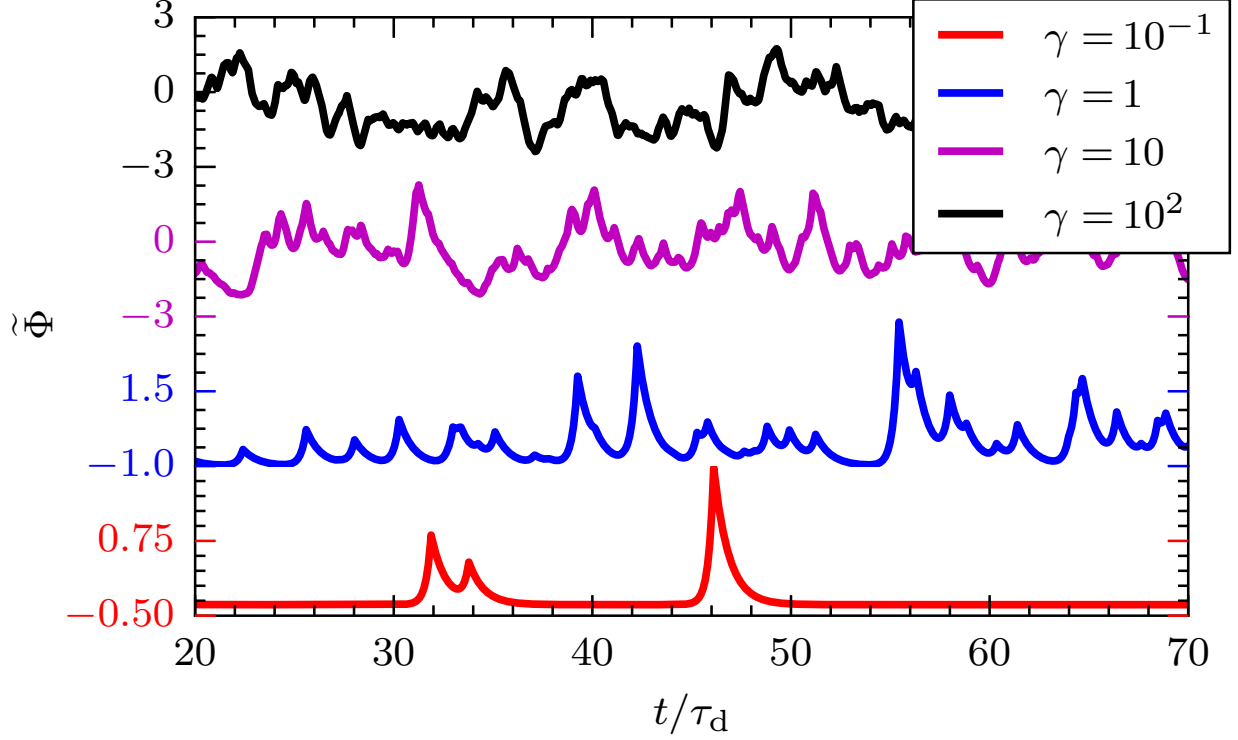


FIG. 2: Realizations of the stochastic process for $\lambda = 1/4$ and various values of γ .

$\tilde{\Phi} = (\Phi - \langle \Phi \rangle) / \Phi_{\text{rms}}$ resembles a normal distribution in the limit $\gamma \rightarrow \infty$, independent of pulse shape and amplitude distribution. In this case, both the skewness S_{Φ} and the excess kurtosis $F_{\Phi} - 3$ vanish.^{11,12} Conversely, for $\gamma \rightarrow 0$, the skewness and kurtosis moments both tend to infinity.

Note that in the case of positive definite amplitudes and the pulse shape in Eq. (9), Φ is non-negative, giving $\tilde{\Phi} \geq -\gamma^{1/2}$. By contrast, a normally distributed random variable has infinite support. The difference between the probability density function of $\tilde{\Phi}$ and a standard normal distribution (the distribution of a normally distributed variable with zero mean and unit standard deviation) due to this discrepancy is negligible, however, since values of $-\gamma^{1/2}$ or less are highly unlikely for a standard normal distribution in the case of $\gamma \gg 1$.

Realizations of this process for various values of γ are shown in Fig. 2. For small γ , the pulses are well separated and the process is strongly intermittent. For large γ , there is significant pulse overlap and realizations of the process resembles random noise, with relatively small and symmetric fluctuations around the mean value. Because of this, as well as the discussion of the skewness and kurtosis given above, the parameter γ can be interpreted as an intermittency parameter for the process.

B. The derivative of the filtered Poisson process

In order to calculate the joint distribution of the process and its derivative, the normalized time derivative is defined by

$$\Theta_K(t) = \frac{\tau_d}{2} \frac{d\Phi_K}{dt} = \sum_{k=1}^{K(T)} A_k \vartheta\left(\frac{t - t_k}{\tau_d}\right), \quad (19)$$

where the pulse shape is given by

$$\vartheta(s) = \frac{1}{2} \frac{d\varphi}{ds} = \frac{1}{2} \begin{cases} (\lambda)^{-1} \exp(s/\lambda), & s < 0, \\ -(1 - \lambda)^{-1} \exp(-s/(1 - \lambda)), & s \geq 0. \end{cases} \quad (20)$$

Where we divide by 2 to fulfill $\int_{-\infty}^{\infty} ds |\vartheta(s)|^4 = 1$. This is another stochastic process of the same type as given in Eq. (7), but with a different pulse shape. Since the process $\Phi(t)$ is stationary, it follows that $\langle \Theta \rangle = 0$. The processes $\Phi(t)$ and $\Theta(t)$ are evidently dependent yet also uncorrelated,

$$\langle \Phi \Theta \rangle = \frac{\tau_d}{4} \frac{d}{dt} \langle \Phi^2 \rangle = 0. \quad (21)$$

In Appendix A it will be shown that in the limit $\gamma \rightarrow \infty$, Φ and Θ become independent.

The lowest order moments of Θ are readily calculated as

$$\langle \Theta \rangle = 0, \quad (22a)$$

$$\Theta_{\text{rms}}^2 = \gamma \langle A \rangle^2 / [4\lambda(1 - \lambda)], \quad (22b)$$

$$S_{\Theta} = 2(1 - 2\lambda) / [\gamma\lambda(1 - \lambda)]^{1/2}, \quad (22c)$$

$$F_{\Theta} = 3 + 6[1 + (1 - 2\lambda)^2 / \lambda(1 - \lambda)] / \gamma. \quad (22d)$$

In the limit of $\lambda \rightarrow 0$ or $\lambda \rightarrow 1$, the moments Θ_{rms} , S_{Θ} and F_{Θ} diverge, meaning the PDF of Θ does not exist in this case. In these limits, the pulse shape in Φ is discontinuous and the derivative of the pulse shape contains delta functions. Thus we require the two-sided exponential waveform to calculate the rate of level crossings. It will later be shown that these limits exist for the rate of level crossings. Thus, while this method cannot calculate the rate of level crossings for a discontinuous signal, the rate still exists.

Using the same approach as in Refs. 12 and 13, the characteristic function of Θ is given by

$$\langle \exp(i\Theta v) \rangle = \left(1 - i \langle A \rangle \frac{v}{2\lambda}\right)^{-\lambda\gamma} \left(1 + i \langle A \rangle \frac{v}{2(1 - \lambda)}\right)^{-(1 - \lambda)\gamma} \quad (23)$$

This characteristic function can be interpreted as originating from two independent gamma distributed variables, one over positive values with shape parameter $\gamma\lambda$ and scale parameter

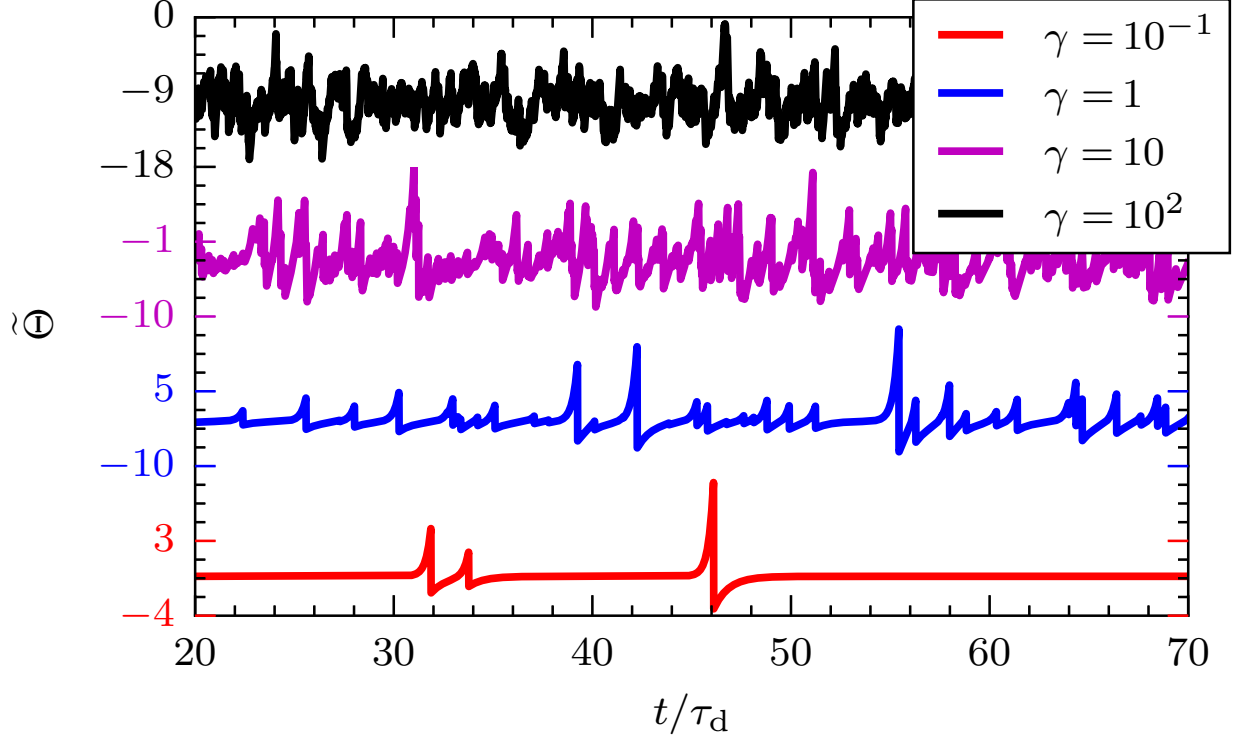


FIG. 3: Realizations of the derivative of the stochastic process for $\lambda = 1/4$ and various values of γ .

$\langle A \rangle / (2\lambda)$, and the other over negative values with shape parameter $\gamma(1 - \lambda)$ and scale parameter $-\langle A \rangle / [2(1 - \lambda)]$. In Fig. 3, realizations for $\tilde{\Theta}$ are presented for $\lambda = 1/4$ and various values of γ . Arrival times and pulse amplitudes are the same as in Fig. 2. Again, the process is intermittent for low values of γ , and resembles random noise for high values of γ . The PDF of this compound process is a convolution of the two gamma distributions, which to the best of the authors knowledge does not have a closed form. Still, the argument in Refs. 12 and 13 applies here as well, and the PDF of Θ resembles a normal distribution in the limit $\gamma \rightarrow \infty$.

By choosing a $\lambda = 1/2$, the waveform for Φ is symmetric. In this case, the characteristic function in Eq. (23) has an inverse transformation, and the corresponding PDF is given by

$$P_{\tilde{\Theta}}(\tilde{\Theta}) = \sqrt{\frac{2\gamma}{\pi}} \frac{2^{-\gamma/2}}{\Gamma(\gamma/2)} \left| \sqrt{\gamma} \tilde{\Theta} \right|^{(\gamma-1)/2} \mathcal{K}_{(\gamma-1)/2} \left(\left| \sqrt{\gamma} \tilde{\Theta} \right| \right), \quad (24)$$

where $\mathcal{K}_a(x)$ is the modified Bessel function of the second kind with parameter a and variable x , given in Ref. 39, Ch. 10.25. Some realizations of this PDF are shown in Fig. 4. For small values of γ , this PDF is sharply peaked around the mean value, while it resembles a normal distribution for large values of γ . The exponential tails of the distribution can be seen for all values of γ , and it

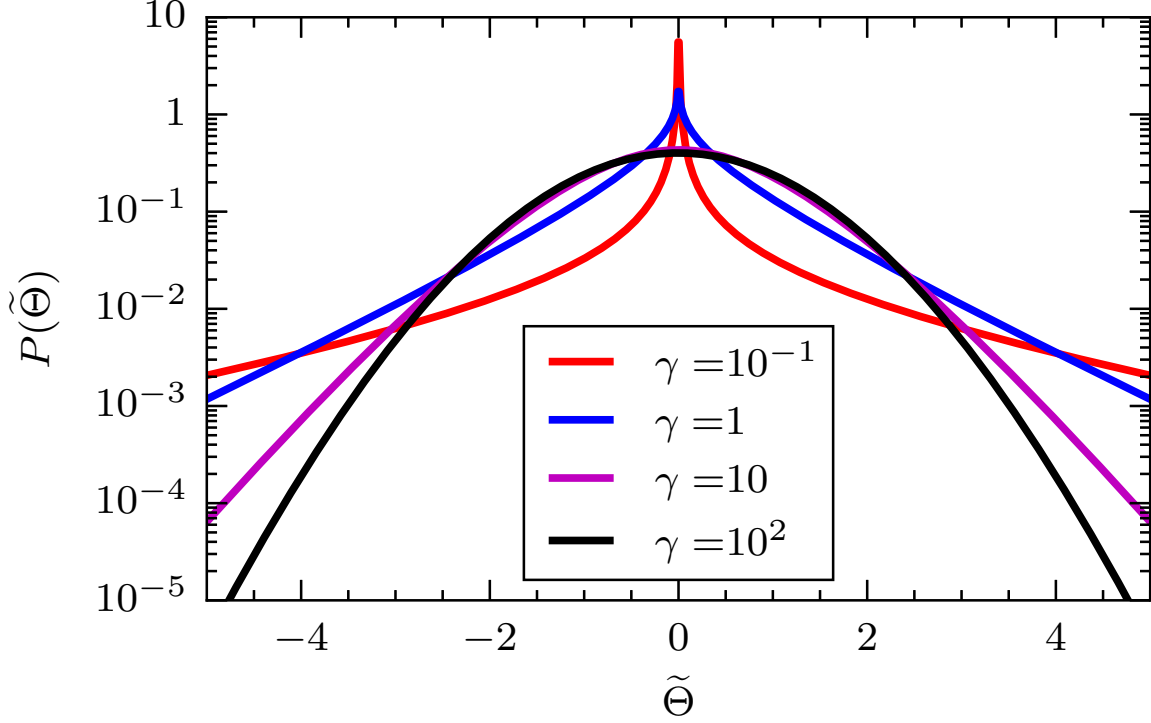


FIG. 4: PDF of the normalized derivative of the shot noise process with $\lambda = 1/2$ and various values of γ .

can be seen from Eq. (23) that Θ is Laplace distributed with mean value $\langle A \rangle$ in the case $\lambda = 1/2$, $\gamma = 2$.

C. The joint PDF of the filtered Poisson process

Using that individual events are uncorrelated and that the number of pulses is Poisson distributed, the joint probability density function of Φ and Θ can be calculated as

$$P_{\Phi\Theta}(\Phi, \Theta) = \frac{1}{(2\pi)^2} \int_{-\infty}^{\infty} du \int_{-\infty}^{\infty} dv \exp(-i\Phi u - i\Theta v) \langle \exp(iu\Phi + iv\Theta) \rangle, \quad (25)$$

where

$$\langle \exp(iu\Phi + iv\Theta) \rangle = \exp \left(\gamma \int_{-\infty}^{\infty} dA P_A(A) \int_{-\infty}^{\infty} ds [\exp(iuA\varphi(s) + ivA\vartheta(s)) - 1] \right) \quad (26)$$

is the joint characteristic function between Φ and Θ . This expression is given in Refs. 24 and 19 for the case of fixed (degenerately distributed) pulse amplitudes, although the generalization is

straightforward. Exchanging the order of integration we find that

$$\langle \exp(iu\Phi + iv\Theta) \rangle = \left[1 - i \langle A \rangle \left(u + \frac{v}{2\lambda} \right) \right]^{-\gamma\lambda} \left[1 - i \langle A \rangle \left(u - \frac{v}{2(1-\lambda)} \right) \right]^{-\gamma(1-\lambda)}. \quad (27)$$

We note that we recover the expression for the characteristic function of Φ in Eq. (14) by setting $v = 0$ in this equation, and we recover the characteristic function of Θ in Eq. (23) by setting $u = 0$. Substituted into Eq. (25), the stationary joint probability density function can be obtained in closed form. We have that

$$P_{\Phi\Theta}(\Phi, \Theta) = \frac{1}{(2\pi)^2} \int_{-\infty}^{\infty} du \int_{-\infty}^{\infty} dv \left\{ \exp(-iu\Phi - iv\Theta) \times \left[1 - i \langle A \rangle \left(u + \frac{v}{2\lambda} \right) \right]^{-\gamma\lambda} \left[1 - i \langle A \rangle \left(u - \frac{v}{2(1-\lambda)} \right) \right]^{-\gamma(1-\lambda)} \right\}. \quad (28)$$

Doing the change of variables $x = \langle A \rangle [u + v/(2\lambda)]$, $y = \langle A \rangle \{u - v/[2(1-\lambda)]\}$ and using the notation

$$\alpha = \frac{\lambda}{\langle A \rangle} [\Phi + 2(1-\lambda)\Theta],$$

$$\beta = \frac{1-\lambda}{\langle A \rangle} (\Phi - 2\lambda\Theta),$$

we can write the joint PDF as

$$P_{\Phi\Theta}(\Phi, \Theta) = \frac{2\lambda(1-\lambda)}{(2\pi \langle A \rangle)^2} \int_{-\infty}^{\infty} dx [1 - ix]^{-\gamma\lambda} \exp(-i\alpha x) \int_{-\infty}^{\infty} dy [1 - iy]^{-\gamma(1-\lambda)} \exp(-i\beta y). \quad (29)$$

The separated integrals can be performed and we find the expression

$$P_{\Phi\Theta}(\Phi, \Theta) = \frac{2\gamma^\gamma \lambda^{\gamma\lambda} (1-\lambda)^{\gamma(1-\lambda)}}{\langle \Phi \rangle^\gamma \Gamma(\gamma\lambda) \Gamma(\gamma(1-\lambda))} \exp\left(-\frac{\gamma\Phi}{\langle \Phi \rangle}\right) [\Phi + 2(1-\lambda)\Theta]^{\gamma\lambda-1} (\Phi - 2\lambda\Theta)^{\gamma(1-\lambda)-1}. \quad (30)$$

This is non-zero only for the limited range $-\Phi/[2(1-\lambda)] < \Theta < \Phi/(2\lambda)$, which follows from the fact that the signal $\Phi(t)$ cannot decrease faster than the rate of decay of individual pulse structures, nor increase slower than the rate of growth of individual pulses. The dependence between Φ and Θ is evident from Eq. (30), since the joint PDF is not separable into a product of the marginal PDFs. As expected, $P_\Phi(\Phi)$ can be recovered by integrating over Θ . Also note that the expression for the joint PDF diverges in the limits $\lambda \rightarrow 0$ and $\lambda \rightarrow 1$, as was the case for the moments and PDF of Θ . As the PDFs of both Φ and Θ resemble normal distributions in the limit $\gamma \rightarrow \infty$ and they are

uncorrelated, the joint probability density function for Φ and Θ resembles the product of two normal distributions, that is, a joint normal distribution with vanishing correlation coefficient. Thus, in the normal limit $\gamma \rightarrow \infty$, the classical Rice formula given by Eq. (2) discussed above is recovered. This is shown explicitly in Appendix A. As in the case of P_Φ , there is a discrepancy between $P_{\Phi\Theta}$ and a joint normal distribution due to the limited region of non-zero values of $P_{\Phi\Theta}$. The domain of non-zero values can be written as $-(\tilde{\Phi} + \gamma^{1/2})/(1 - \lambda) < \tilde{\Theta}/\sqrt{\lambda(1 - \lambda)} < (\tilde{\Phi} + \gamma^{1/2})/\lambda$ where $\tilde{\Theta} = \Theta/\Theta_{\text{rms}}$. For standard normally distributed variables, values outside of this domain are highly unlikely in the case of $\gamma \gg 1$, and this discrepancy is in practice negligible.

The joint distribution $P_{\Phi\Theta}(\Phi, \Theta)$ is presented in Fig. 5 for $\gamma = \{10^{-1}, 1, 10\}$ and $\lambda = \{1/4, 1/2\}$. It should be noted that logarithmic scaling is used for $\gamma = 10^{-1}$ and 1, while linear scaling is used for $\gamma = 10$. Also $\gamma = 1$, $\lambda = 1/2$ uses the numerical value $\gamma = 1.01$ to avoid singularities in the computation. The white area in all figures are the regions where $P_{\Phi\Theta}$ vanishes, as given by Eq. (30). The joint distribution for $\gamma \leq 1$ diverges at $\Phi = 0$ and $\Theta = 0$, since the pulses arrive rarely enough for the signal to fall close to zero for long time durations. In this case, the signal is very likely to decay undisturbed at the rate of individual pulses, explaining the increased value of the joint distribution near the line $\Theta = -\Phi/[2(1 - \lambda)]$. The joint distribution for $\gamma = 10$ is unimodal, since significant pulse overlap causes a wider range of values for Θ to be likely for a given value of Φ .

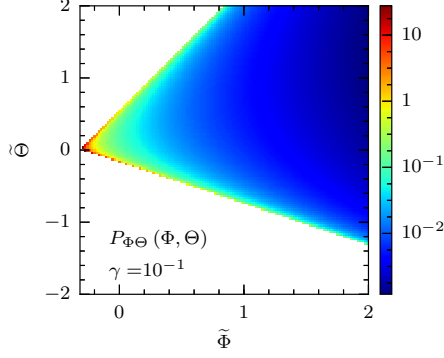
III. EXCESS TIME STATISTICS

In this section we present the rate of threshold crossings and average time above threshold for the shot noise process. Limits of one-sided exponential waveform, and low and high intermittency are explored and compared to previous works. In the end, we discuss the rate of level crossings for a shot noise process with Laplace distributed amplitudes.

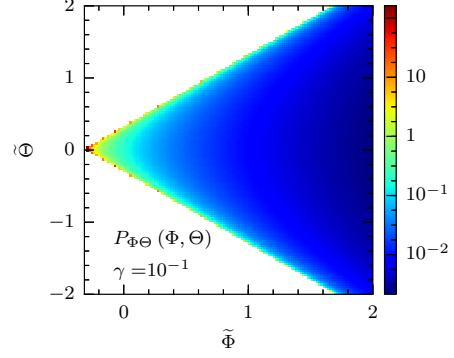
A. Formulation of excess time statistics

The rate of up-crossings above a threshold Φ is now readily calculated from Eqs. (1) and (30) as

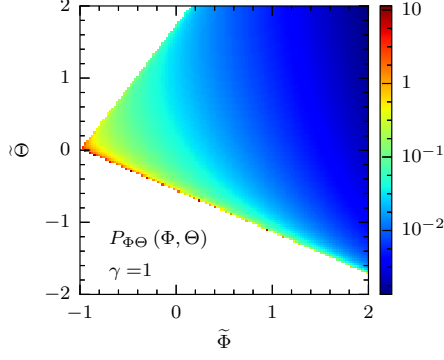
$$\frac{\tau_d}{T} X(\Phi) = 2 \int_0^\infty d\Theta \Theta P_{\Phi\Theta}(\Phi, \Theta) = \frac{\lambda^{\gamma\lambda-1} (1 - \lambda)^{\gamma(1-\lambda)-1}}{\gamma \Gamma(\gamma\lambda) \Gamma(\gamma(1 - \lambda))} \left(\frac{\gamma\Phi}{\langle\Phi\rangle} \right)^\gamma \exp\left(-\frac{\gamma\Phi}{\langle\Phi\rangle}\right), \quad (31)$$



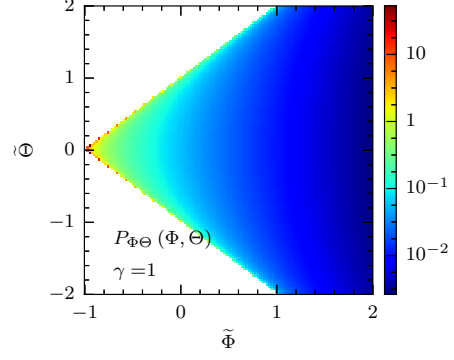
(a) Joint PDF for $\gamma = 10^{-1}$ and $\lambda = 1/4$.



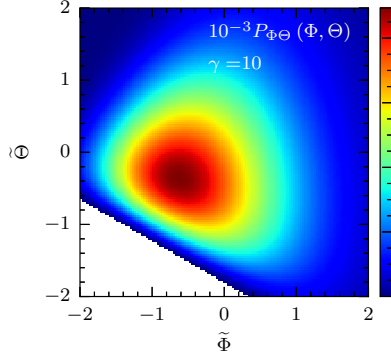
(b) Joint PDF for $\gamma = 10^{-1}$ and $\lambda = 1/2$.



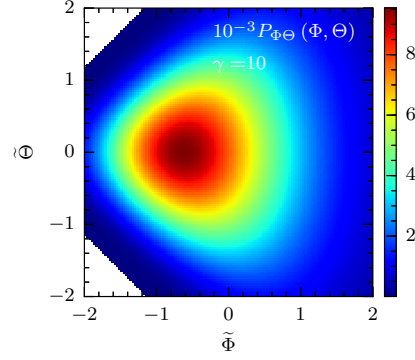
(c) Joint PDF for $\gamma = 1$ and $\lambda = 1/4$.



(d) Joint PDF for $\gamma = 1$ and $\lambda = 1/2$.



(e) Joint PDF for $\gamma = 10$ and $\lambda = 1/4$.



(f) Joint PDF for $\gamma = 10$ and $\lambda = 1/2$.

FIG. 5: Joint PDF between $\tilde{\Phi}$ and $\tilde{\Theta}$ for various values of γ and λ .

which, together with the complementary cumulative distribution function in Eq. (13), gives the average time above the threshold

$$\frac{1}{\tau_d} \langle \Delta T \rangle (\Phi) = \frac{\gamma \Gamma(\gamma \lambda) \Gamma(\gamma(1-\lambda))}{\lambda^{\gamma \lambda - 1} (1-\lambda)^{\gamma(1-\lambda) - 1}} Q\left(\gamma, \frac{\gamma \Phi}{\langle \Phi \rangle}\right) \left(\frac{\gamma \Phi}{\langle \Phi \rangle}\right)^{-\gamma} \exp\left(\frac{\gamma \Phi}{\langle \Phi \rangle}\right). \quad (32)$$

Note that both Eqs. (31) and (32) can be written as a pre factor depending on γ and λ multiplied by a function of γ and

$$\gamma\Phi/\langle\Phi\rangle = \sqrt{\gamma}\tilde{\Phi} + \gamma. \quad (33)$$

This indicates that the functional shape of both equations with threshold level depends only on the intermittency parameter γ , while the total value of the functions depends on both γ and λ . By contrast, the complementary cumulative distribution function given by Eq. (13) does not depend on λ .

The rate of up-crossings as function of the threshold level for various values of γ is presented in Fig. 6. Full lines show the case of $\lambda = 1/2$, while dashed lines show the rate of level crossings in the limit $\lambda \rightarrow 0$. The expression for this limit will be discussed further in Sec. III B. The number of crossings is evidently proportional to the length of the time series T and inversely proportional to the pulse duration τ_d . The rate of threshold crossings is highest for thresholds close to the mean value of the process in all cases. In the normal regime $\gamma \gg 1$, there are few crossings for threshold levels much smaller or much larger than the mean value due to the low probability of large-amplitude fluctuations. The rate of level crossings is therefore a narrow Gaussian function in this limit. In the strong intermittency regime, $\gamma \ll 1$, the signal spends most of the time close to zero value, and virtually any pulse arrival will give rise to a level crossing for finite threshold values. As seen in Fig. 6, the rate of level crossings approaches a step function in this limit. For $\lambda = 1/2$, the rate of level crossings at the mean value, $\tilde{\Phi} = 0$, approaches a definite value. In Sec. III C this value is shown to be $1/\pi$. In contrast, there is no limiting value for $\lambda = 0$. $X(\tilde{\Phi} = 0) \rightarrow \infty$ as $\gamma \rightarrow \infty$, as will be shown in Sec. III C.

The average time above threshold is presented in Fig. 7 for various values of γ . Full lines show the case of $\lambda = 1/2$, while dashed lines show the average time above threshold in the limit $\lambda \rightarrow 0$. While both the rate of threshold crossings and the fraction of time above threshold vary qualitatively as γ changes, the shape of the average time above threshold is fairly similar. In all cases the average excess time decreases monotonically with the threshold level, with a fast drop for small threshold values. This is followed by a slow tapering off for large threshold values. For the range of intermittency parameters considered here, the average excess time is of the order of the pulse duration or shorter for large threshold values. For $\lambda \rightarrow 0$, the average time above threshold decreases by about half a decade for each tenfold increase in γ , but the functional shape varies little. For $\lambda = 1/2$, the average time above threshold approaches the Rice result, as will be shown in Sec. III C. It can be shown that for given γ and λ , $\langle\Delta T\rangle/\tau_d$ scales as $1/\tilde{\Phi}$ in the limit $\tilde{\Phi} \rightarrow \infty$. As

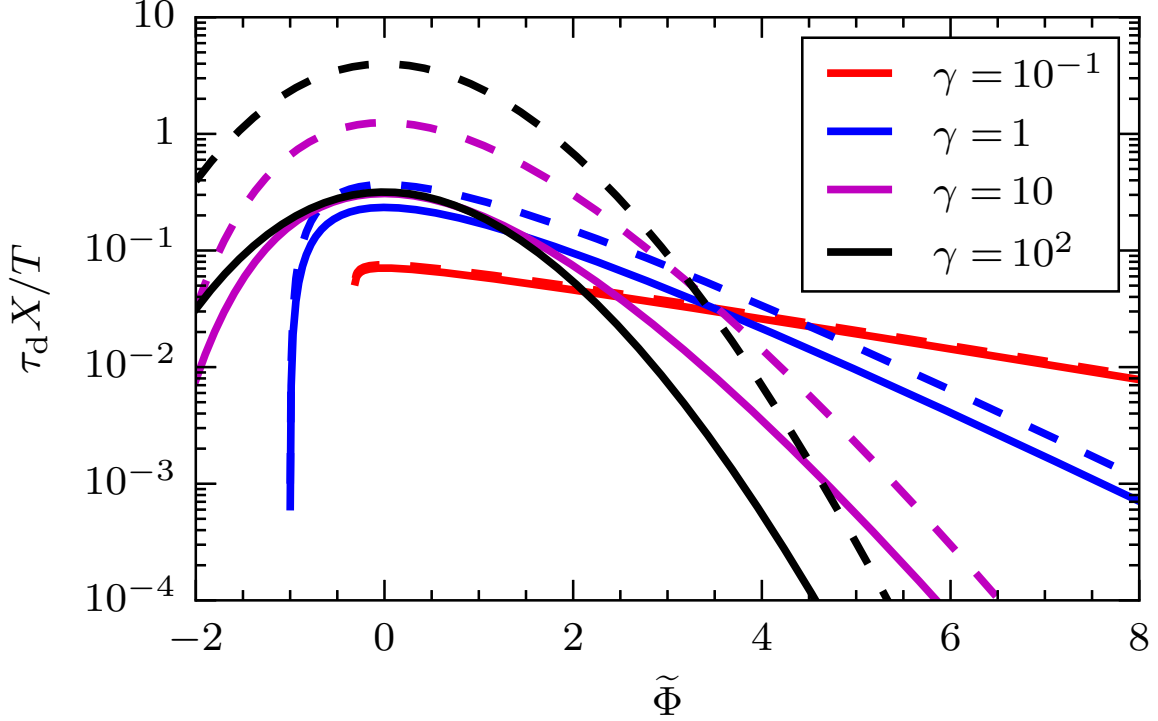


FIG. 6: The rate of up-crossings for the stochastic process with $\lambda = 1/2$ (full lines), $\lambda = 0$ (dashed lines) and various values of γ .

the threshold value increases above the mean signal value, up-crossings of the threshold become fewer while the signal spends less time in total above the threshold. Evidently these two effects nearly cancel, and the average excess time decreases slowly with increasing threshold level.

B. Limit of the one-sided waveform

As stated in Sec. II C, the limit of the one-sided exponential waveform does not exist for P_Θ or $P_{\Phi\Theta}$. This is due to the fact that the waveform Φ is discontinuous in this case, and therefore second and higher order moments of its derivative cannot be computed. However, the rate of level crossings for the discontinuous process still exists, and has been discussed by e.g. Refs. 27, 32, and 34. Taking the limits $\lambda \rightarrow 0$ and $\lambda \rightarrow 1$ give the same results, and yield

$$\frac{\tau_d}{T} X(\Phi) = \frac{1}{\Gamma(\gamma)} \left(\frac{\gamma \Phi}{\langle \Phi \rangle} \right)^\gamma \exp \left(-\frac{\gamma \Phi}{\langle \Phi \rangle} \right). \quad (34)$$

This result was also obtained by Ref. 34 by considering the Fourier transform of the number of level crossings. Since the complementary CDF of Φ does not depend on λ , the total time the signal

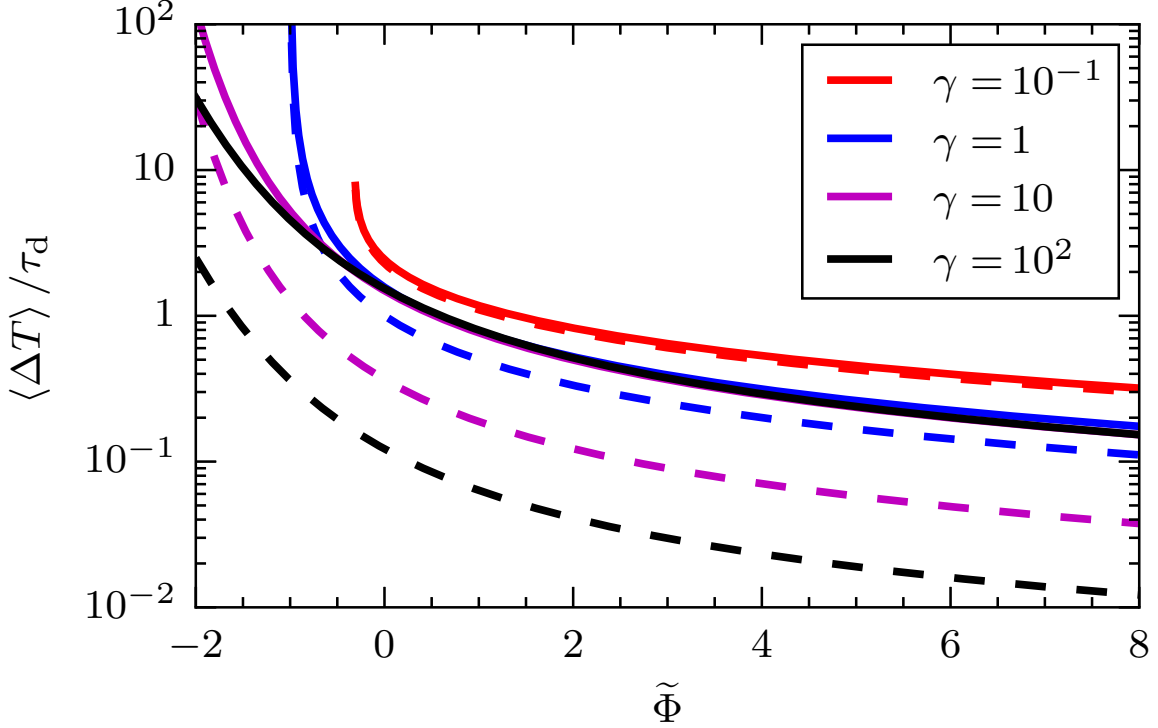


FIG. 7: The average time above threshold for the stochastic process with $\lambda = 1/2$ (full lines), $\lambda = 0$ (dashed lines) and various values of γ .

spends above threshold remains unchanged, and the average time above threshold is simply

$$\frac{1}{\tau_d} \langle \Delta T \rangle (\Phi) = \Gamma(\gamma) Q \left(\gamma, \frac{\gamma \Phi}{\langle \Phi \rangle} \right) \left(\frac{\gamma \Phi}{\langle \Phi \rangle} \right)^{-\gamma} \exp \left(\frac{\gamma \Phi}{\langle \Phi \rangle} \right). \quad (35)$$

The functional shape of Eqs. (34) and (35) are the same as in the full expressions Eqs. (31) and (32), since λ only appears in the prefactor of the expressions. The approach discussed in Ref. 32 also leads to the results presented in this section, although they are not explicitly given in the reference.

C. The normal limit

In the limit of large γ , the expression for $X(\Phi)$ can be simplified and shown to be equal to the case for a normally distributed process. Using Stirling's approximation for the Gamma functions in Eq. (31), we have in the case $\gamma \gg 1$:

$$\lim_{\gamma \rightarrow \infty} \Gamma(\gamma \lambda) \Gamma(\gamma(1 - \lambda)) = \lim_{\gamma \rightarrow \infty} 2\pi \gamma^{\gamma-1} \lambda^{\gamma \lambda - 1/2} (1 - \lambda)^{\gamma(1-\lambda) - 1/2} \exp(-\gamma). \quad (36)$$

Inserting this result into Eq. (31), and using the normalized threshold in Eq. (33), the rate of crossings in the non-intermittent case $\gamma \gg 1$ can be written as

$$\lim_{\gamma \rightarrow \infty} \frac{\tau_d}{T} X(\tilde{\Phi}) = \lim_{\gamma \rightarrow \infty} \frac{1}{2\pi\sqrt{\lambda(1-\lambda)}} \left(\frac{\tilde{\Phi}}{\gamma^{1/2}} + 1 \right)^\gamma \exp\left(-\gamma^{1/2}\tilde{\Phi}\right). \quad (37)$$

By setting $\beta = 0$ and $\lambda = 1$ in Eq. (A6), we have that

$$\lim_{\gamma \rightarrow \infty} \left(\tilde{\Phi}/\gamma^{1/2} + 1 \right)^\gamma \exp\left(-\gamma^{1/2}\tilde{\Phi}\right) = \exp\left(-\tilde{\Phi}^2/2\right), \quad (38)$$

and the rate of level crossings in the limit $\gamma \rightarrow \infty$ can be written as

$$\lim_{\gamma \rightarrow \infty} \frac{\tau_d}{T} X(\tilde{\Phi}) = \frac{1}{2\pi\sqrt{\lambda(1-\lambda)}} \exp\left(-\tilde{\Phi}^2/2\right). \quad (39)$$

This expression is equal to Eq. (4), when using Φ_{rms} from Eq. (18b) and $\dot{\Phi}_{\text{rms}} = 2\Theta_{\text{rms}}/\tau_d$ from Eq. (22b). As mentioned in the discussion for Fig. 6, in the case of $\lambda = 1/2$, we have that $\lim_{\gamma \rightarrow \infty} \tau_d X(\tilde{\Phi} = 0)/T = 1/\pi$.

In Appendix B, it is shown that

$$\lim_{\gamma \rightarrow \infty} Q\left(\gamma, \sqrt{\gamma}\tilde{\Phi} + \gamma\right) = \frac{1}{2} \text{erfc}\left(\frac{\tilde{\Phi}}{\sqrt{2}}\right), \quad (40)$$

and the expression for the average time above threshold in Eq. (32) can be shown to be equivalent to the expression in Eq. (6) in the case $\gamma \rightarrow \infty$. We note that for $\lambda = 1/2$, $\lim_{\gamma \rightarrow \infty} \langle \Delta T \rangle (\tilde{\Phi} = 0)/\tau_d = \pi/2$.

Starting from Eq. (34) and going through the same procedure as above, we have in the cases $\lambda = 0$ and $\lambda = 1$

$$\lim_{\gamma \rightarrow \infty} \frac{\tau_d}{T} \frac{X(\tilde{\Phi})}{\sqrt{\gamma}} = \frac{1}{\sqrt{2\pi}} \exp\left(-\tilde{\Phi}^2/2\right). \quad (41)$$

There is a clear discrepancy between Eqs. (39) and (41), suggesting a qualitative difference between a continuous and discontinuous pulse shape. This result is in agreement with the careful analysis in Ref. 34. The rate of level crossings is much higher for a process with jumps in the pulse shape (and continues to increase with the square root of γ as γ increases). No matter how strong the pulse overlap is, the jumps are much more likely to trigger threshold crossings than the continuous pulses.

We also note that the average time above threshold can be written as

$$\lim_{\gamma \rightarrow \infty} \frac{\langle \Delta T \rangle}{\tau_d} \sqrt{\gamma} = \sqrt{\frac{\pi}{2}} \text{erfc}\left(\frac{\tilde{\Phi}}{\sqrt{2}}\right) \exp\left(\frac{\tilde{\Phi}^2}{2}\right). \quad (42)$$

Just as the rate of level crossings increases without bound for increasing pulse overlap in the cases $\lambda = 0$ and $\lambda = 1$, the average time above threshold decreases with increasing γ . Thus, in the normal limit, the process is characterized by many, short threshold crossings. In the case of discontinuous pulse shape, the derivative of the process does not exist, and the method we have used to find the rate of threshold crossings is not valid (but still gives results in agreement with other methods). In this case, Rice's formula, Eq. (6) does not exist for the process (as Θ_{rms} does not exist). Thus, the rate of pulse arrivals will always play a role in the expression.

D. The strong intermittency limit

We will now investigate the limit of $\gamma \rightarrow 0$, where we can neglect super-position of pulses, such that each pulse appears as one, and only one, burst in the resulting signal. In this section, we will use $\Phi / \langle A \rangle$ instead of the expressions in Eq. (33), to avoid γ where possible. In the previous section, $\tilde{\Phi}$ approached a standard, normally distributed variable. Here, $\tilde{\Phi}$ approaches a random variable with infinite skewness and flatness, and the advantage of the normalization is diminished. In the limit $\gamma \rightarrow 0$, we can find the number of threshold crossings, the average time above threshold and even the distribution of time above threshold for each up-crossing without going through the joint PDF of $\Phi(t)$ and $\Theta(t)$.

When the pulses are completely separated, the total number of upward crossings above the threshold must be the same as the total number of pulses with amplitude higher than the threshold value. Therefore, the total number of up-crossings can be written as

$$\lim_{\gamma \rightarrow 0} \frac{X(\Phi)}{\gamma} = \sum_{K=0}^{\infty} P_K(K) \frac{K}{\gamma} \int_{\Phi/\varphi_{\max}}^{\infty} dA P_A(A) = \frac{\langle K \rangle}{\gamma} \int_{\Phi}^{\infty} dA \frac{1}{\langle A \rangle} \exp\left(-\frac{A}{\langle A \rangle}\right) = \frac{T}{\tau_d} \exp\left(-\frac{\Phi}{\langle A \rangle}\right), \quad (43)$$

where $\langle K \rangle = T/\tau_w = \gamma T/\tau_d$ and φ_{\max} is the largest positive value of φ . For the exponential pulse shape in Eq. (9), $\varphi_{\max} = \varphi(0) = 1$. This expression can also be reached by taking the limit $\gamma \rightarrow 0$ in either Eqs. (31) or (34), suggesting that the number is the same for a continuous and a discontinuous pulse. This can be explained by the fact that each sufficiently large-amplitude pulse triggers one crossing above the threshold, and this is independent of the pulse shape.

Using the complementary CDF from Eq. (13), we have

$$\lim_{\gamma \rightarrow 0} \frac{1}{T} \frac{1 - C_{\Phi}(\Phi)}{\gamma} = \lim_{\gamma \rightarrow 0} \frac{Q(\gamma, \Phi/\langle A \rangle)}{\gamma} = \Gamma\left(0, \frac{\Phi}{\langle A \rangle}\right), \quad (44)$$

where $\Gamma(s, x)$ is the upper incomplete Gamma function [REF] with parameter s and variable x . Estimating $\langle \Delta T \rangle$ by $(1 - C_\Phi)/X$, given by Eqs. (43) and Eq. (44), we find that the average time above threshold is given by

$$\lim_{\gamma \rightarrow 0} \frac{1}{\tau_d} \langle \Delta T \rangle (\Phi) = \exp \left(\frac{\Phi}{\langle A \rangle} \right) \Gamma \left(0, \frac{\Phi}{\langle A \rangle} \right). \quad (45)$$

The rate of level crossings, Eq. (43), and the fraction of time above threshold, Eq. (44), both decay as γ in the limit $\gamma \rightarrow 0$. Since the dependency of these two expressions on γ is the same, the average time the signal spends above the threshold is independent of γ .

Before discussing the PDF of ΔT , we will take a brief look at a shot noise process with a different amplitude distribution.

E. Laplace distributed amplitudes

The Laplace distribution can be written a few different ways, see e.g Refs. 41 and 42. We will give it as

$$P_A(A; \alpha, \kappa) = \frac{1}{2\alpha} \begin{cases} \exp \left(-\frac{A}{2\alpha(1-\kappa)} \right), & A > 0 \\ \exp \left(\frac{A}{2\alpha\kappa} \right), & A < 0 \end{cases}, \quad (46)$$

where $\alpha > 0$ is a scale parameter and $0 < \kappa < 1$ is an asymmetry parameter. For $\kappa = 1/2$, the symmetric Laplace distribution is recovered. The filtered Poisson process with Laplace distributed amplitudes has a PDF on closed form^{6,32}. Inserting the PDF for the Laplace distribution into Eq. (26) and separating the integral over the amplitude distribution into positive and negative amplitudes, we can proceed as in Sec. II C. We find that

$$\begin{aligned} \langle \exp(iu\Phi + iv\Theta) \rangle &= \left[1 + 2\alpha i\kappa \left(u - \frac{v}{2(1-\lambda)} \right) \right]^{-\gamma\kappa(1-\lambda)} \left[1 + 2\alpha i\kappa \left(u + \frac{v}{2\lambda} \right) \right]^{-\gamma\kappa\lambda} \times \\ &\times \left[1 - 2\alpha i(1-\kappa) \left(u - \frac{v}{2(1-\lambda)} \right) \right]^{-\gamma(1-\kappa)(1-\lambda)} \left[1 - 2\alpha i(1-\kappa) \left(u + \frac{v}{2\lambda} \right) \right]^{-\gamma(1-\kappa)\lambda}. \end{aligned} \quad (47)$$

The characteristic function given in Eq. (27) is a special case of the equation above, with $\kappa = 0$ and $\alpha = \langle A \rangle / 2$. Using the same basic approach as in Sec. II C, we can write the joint PDF as the product of two integrals,

$$\begin{aligned} P_{\Phi\Theta}(\Phi, \Theta) &= \frac{2\lambda(1-\lambda)}{(2\alpha)^2} \mathcal{I} \left(\frac{\lambda}{2\alpha} \Phi + \frac{2\lambda(1-\lambda)}{2\alpha} \Theta; \kappa, \gamma\lambda \right) \times \\ &\times \mathcal{I} \left(\frac{1-\lambda}{2\alpha} \Phi - \frac{2\lambda(1-\lambda)}{2\alpha} \Theta; \kappa, \gamma(1-\lambda) \right), \end{aligned} \quad (48)$$

where

$$\mathcal{I}(x; a, b) = \frac{1}{2\pi} \int_{-\infty}^{\infty} du \exp(-ixu) (1 - i(1-a)u)^{-b(1-a)} (1 + iau)^{-ba} \quad (49)$$

for the variable x and parameters $0 < a < 1$ and $b > 0$. This integral can be interpreted as the PDF of a sum of two Gamma distributed variables, one with positive amplitudes, scale parameter $(1-a)$ and shape parameter $b(1-a)$, and the other over negative amplitudes with scale parameter a and shape parameter ba . The full joint PDF of Φ and Θ is thus the product of two such distributions with interlocked variables. Note that unlike the joint PDF in the case of exponentially distributed amplitudes, given by Eq. (30), the distribution in Eq. (48) is positive definite for the entire domain. This is due to the pulses being able to take both positive and negative values, so there are no bounds on the maximal or minimal growth or decay of the signal.

We will now consider the rate of level crossings for a special case of the joint PDF given in Eq. (48), with symmetric Laplace distributed amplitudes, $\kappa = 1/2$, and one-sided exponential pulse shape, $\lambda \rightarrow 0$. The integral in Eq. (49) has a closed form for $a = 1/2$;

$$\mathcal{I}(x; 1/2, b) = \frac{2|x|^{(b-1)/2}}{\sqrt{\pi}\Gamma(b/2)} \mathcal{K}_{(b-1)/2}(2|x|), \quad (50)$$

Note that this implies that Eq. (24) can be written as $P_{\tilde{\Theta}}(\tilde{\Theta}) = 2\mathcal{I}(\sqrt{\gamma}\tilde{\Theta}/2, 1/2, \gamma)/\sqrt{\gamma}$. Inserting Eq. (48) with $\kappa = 1/2$ into the expression for the rate of threshold crossings Eq. (1) and taking the limit $\lambda \rightarrow 0$, we have the simplified expression

$$\frac{\tau_d}{T} X(\Phi) = \frac{\gamma}{\sqrt{\pi}\Gamma(\gamma/2)} \int_0^{\infty} du \left| u - \frac{\Phi}{2\alpha} \right|^{(\gamma-1)/2} \exp(-2u) \mathcal{K}_{(\gamma-1)/2} \left(2 \left| u - \frac{\Phi}{2\alpha} \right| \right). \quad (51)$$

The same expression can be found by using the method given in Ref. 32. For half-integer parameter, the Bessel functions are expressible with elementary functions, see Ref. 39, Ch. 10.47, 10.49. This corresponds to even γ , so for e.g. $\gamma = 2$ we have $\mathcal{K}_{1/2}(x) = \sqrt{\pi/2} \exp(-x)/\sqrt{x}$. This gives

$$\frac{\tau_d}{T} X(\Phi) = \frac{1}{4} \exp \left(-\sqrt{2} |\tilde{\Phi}| \right) \begin{cases} 1 + 2\sqrt{2}\tilde{\Phi} & \tilde{\Phi} > 0 \\ 1 & \tilde{\Phi} < 0 \end{cases}, \quad (52)$$

where $\tilde{\Phi} = (\Phi - \langle \Phi \rangle)/\Phi_{\text{rms}} = \Phi/\Phi_{\text{rms}} = \Phi/\sqrt{2\alpha}$. In contrast, finding the rate of threshold crossings in the case of exponentially distributed amplitudes, with $\lambda \rightarrow 0$ and $\gamma = 2$, we find from Eq. (34), with the normalization in Eq. (33):

$$\frac{\tau_d}{T} X(\Phi) = \left(\sqrt{2}\tilde{\Phi} + 2 \right)^2 \exp \left(-\sqrt{2}\tilde{\Phi} - 2 \right). \quad (53)$$

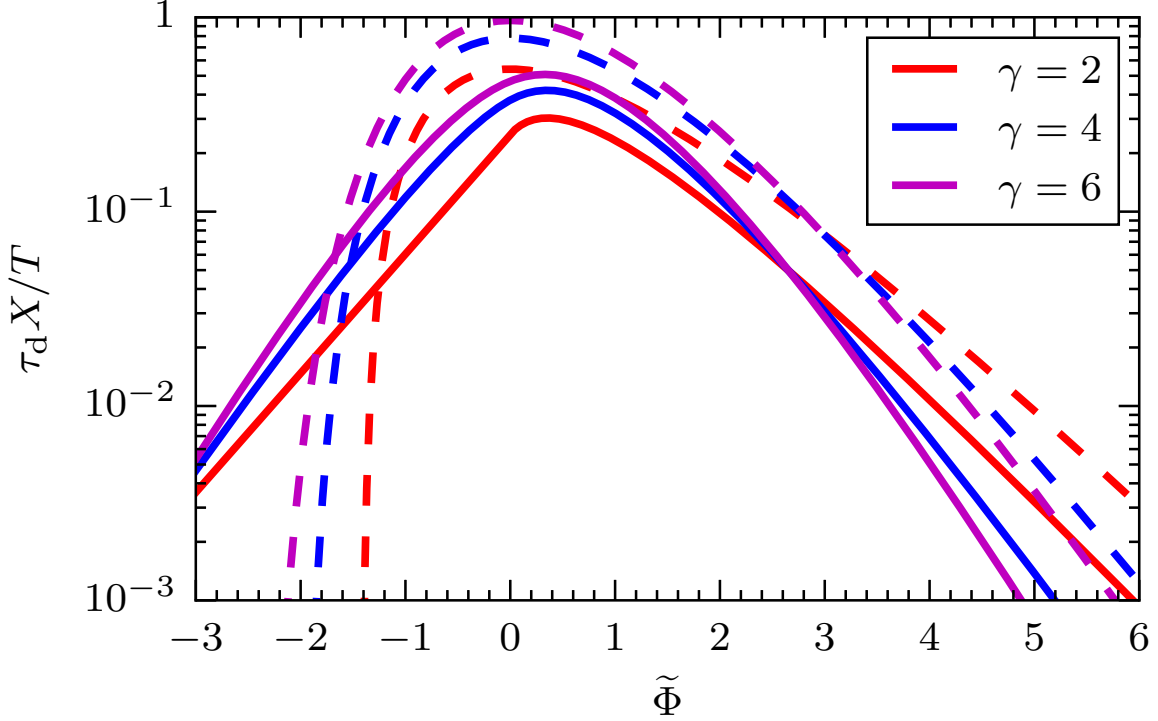


FIG. 8: Rate of level crossings for a shot noise process with symmetric Laplace distributed amplitudes (full lines) and exponentially distributed amplitudes (dashed lines), in the limit of one-sided pulses.

In Fig. 8, the rate of level crossings for the shot noise process with symmetric Laplace distributed amplitudes (full lines) is compared to the rate of level crossings for the shot noise process with exponentially distributed amplitudes (dashed lines), both in the limit $\lambda \rightarrow 0$. It is evident that for the same number of pulse arrivals, the rate of threshold crossings for positive values is larger for the shot noise process with exponentially distributed amplitudes than for Laplace distributed amplitudes. This is due to every pulse in the exponential case potentially contributing to a threshold crossing, while negative pulses in the Laplace case do not. Even though the rate of pulse arrivals is the same, there are more positive pulses in the exponential case.

IV. THE PDF OF EXCESS TIMES

In this section, we will investigate the PDF of the time spent above threshold. In the strong intermittency limit, we can find an analytical expression for this PDF. In the normal limit, with $\lambda \rightarrow 0$, an analytical expression can also be found, but will depend explicitly on γ . In the following,

we will use L as the threshold value.

A. The strong intermittency limit

In this section, we will derive the PDF of the time above threshold in the case of no pulse overlap (that is, the limit $\gamma \rightarrow 0$), and for brevity, we will not include the limit in the following. We will also use $\varphi_{\max} = \varphi(0) = 1$. Generalization to arbitrary φ_{\max} is done by replacing the threshold L by L/φ_{\max} .

For a given pulse with amplitude $A > L$, the signal spends a time ΔT above the threshold. With the two-sided exponential waveform, ΔT can be divided into a time before the peak, ΔT_r , and a time after the peak, ΔT_f . Assuming the pulse arrives at time $t = 0$, the pulse crosses the threshold L upwards at time ΔT_r :

$$L = A \exp\left(\frac{\Delta T_r}{\lambda \tau_d}\right),$$

$$\Delta T_r = -\lambda \tau_d \ln\left(\frac{A}{L}\right),$$

and the pulse crosses the threshold downwards at time ΔT_f

$$L = A \exp\left(-\frac{\Delta T_f}{(1-\lambda)\tau_d}\right),$$

$$\Delta T_f = (1-\lambda)\tau_d \ln\left(\frac{A}{L}\right).$$

Thus, the total time that the pulse spends above the threshold is

$$\Delta T = \Delta T_f - \Delta T_r = \tau_d \ln\left(\frac{A}{L}\right), \quad (54)$$

and the pulse asymmetry plays no further role. ΔT is always positive, since $A > L$ for all the relevant amplitudes. Using that A is exponentially distributed with mean value $\langle A \rangle$, the conditional PDF of A given that $A > L$, is given by the truncated distribution⁴³

$$P_A(A|A > L) = \frac{1}{\langle A \rangle} \exp\left(-\frac{A-L}{\langle A \rangle}\right), \quad A > L. \quad (55)$$

Changing the random variable from A to ΔT and ensuring proper normalization for the PDF of excess times gives

$$P_{\Delta T}(\Delta T) = \frac{1}{\tau_d} \frac{L}{\langle A \rangle} \exp\left(\frac{1}{\tau_d} \Delta T\right) \exp\left(-\frac{L}{\langle A \rangle} \left[\exp\left(\frac{1}{\tau_d} \Delta T\right) - 1\right]\right), \quad \Delta T > 0. \quad (56)$$

This is the so-called Gompertz distribution with parameters $L/(\langle A \rangle \tau_d)$ and $1/\tau_d$, see e.g. Ref. 44, Ch. 10.20. The mean value of the Gompertz distribution can be calculated as

$$\langle \Delta T \rangle (L) = \tau_d \exp \left(\frac{L}{\langle A \rangle} \right) \Gamma \left(0, \frac{L}{\langle A \rangle} \right), \quad (57)$$

which is equivalent to the expression in Eq. (45). The PDF of ΔT will be compared to synthetic data in Sec. V A.

B. The normal limit

It can be shown^{11–13} that the shot noise process approaches a normally distributed process in the limit $\gamma \gg 1$. In the case of $\lambda \rightarrow 0$, $\gamma \gg 1$, the rescaled process $\tilde{\Phi}$ is characterized by a Gaussian probability distribution and an exponential auto-correlation function. The statistical properties of a normally distributed random process are completely described by its PDF and autocorrelation function⁴⁵, and the process is thus statistically identical to any process with a standard normal distribution and exponential auto-correlation function generated by different means.

Much work has been done to elucidate the level crossing statistics and time above or below threshold for an Ornstein-Uhlenbeck (OU) process^{30,33}. We give the OU-process in our notation as

$$dX(t) = -\frac{1}{\tau_d} X(t) dt + \sqrt{\frac{2}{\tau_d}} dW(t), \quad (58)$$

where dW is a standard Wiener process. We give the known initial value as $X(0) = x_0 > 0$. For $t \rightarrow \infty$, this process is stationary and has a standard normal distribution and an exponential autocorrelation function with e-folding time τ_d . It is thus identical to $\tilde{\Phi}$ with the conditions described above.

For the case of zero threshold, Ref. 33 gives the PDF of time above threshold ΔT (and a discussion of references) as

$$P_{\Delta T}(\Delta T|x_0) = \frac{x_0}{2\tau_d\sqrt{\pi}} \sinh(\Delta T/\tau_d)^{-3/2} \exp \left(\frac{\Delta T}{2\tau_d} - \frac{x_0^2 \exp(-\Delta T/\tau_d)}{4 \sinh(\Delta T/\tau_d)} \right). \quad (59)$$

The initial value $x_0 > 0$ can be identified as the rescaled value of the signal below the threshold plus the value of the pulse which brought the signal above the threshold. If the initial value is Φ_0 , the relationship between x_0 and Φ_0 is

$$\Phi_0 = \Phi_{\text{rms}} x_0 + \langle \Phi \rangle, \quad (60)$$

And we show in Appendix C that for a threshold value L , Φ_0 has a truncated exponential distribution

$$P_{\Phi_0}(\Phi_0|L) = \frac{1}{\langle A \rangle} \exp\left(-\frac{\Phi_0 - L}{\langle A \rangle}\right), \quad \Phi_0 > L. \quad (61)$$

With x_0 given above and the threshold being the zero crossing of $\tilde{\Phi}$, which corresponds to crossing the mean value of Φ (as was also commented by Ref. 33, crossing any stationary mean value is statistically equivalent to crossing the stationary mean value 0), we have

$$P_{x_0}(x_0) = \Phi_{\text{rms}} P_{\Phi_0}(\Phi_{\text{rms}} x_0 + \langle \Phi \rangle | L = \langle \Phi \rangle) = \sqrt{\gamma} \exp(-\sqrt{\gamma} x_0), \quad x_0 > 0. \quad (62)$$

Thus the full PDF of ΔT can be shown to be

$$\begin{aligned} P_{\Delta T}(\Delta T) &= \int_0^\infty dx_0 P_{\Delta T}(\Delta T|x_0) P_{x_0}(x_0) \\ &= \frac{1}{\tau_d} \sqrt{\frac{2\gamma}{\pi}} \exp\left(\frac{2\Delta T}{\tau_d}\right) \left[\frac{1}{\sqrt{\exp(2\Delta T/\tau_d) - 1}} \right. \\ &\quad \left. - \sqrt{\frac{\pi\gamma}{2}} \exp\left(\frac{\gamma(\exp(2\Delta T/\tau_d) - 1)}{2}\right) \operatorname{erfc}\left(\sqrt{\frac{\gamma(\exp(2\Delta T/\tau_d) - 1)}{2}}\right) \right]. \end{aligned} \quad (63)$$

Changing variables to $\tau = \gamma [\exp(2\Delta T/\tau_d) - 1] / 2$, this PDF can be written more compactly as

$$P_\tau(\tau) = \frac{1}{\sqrt{\pi\tau}} - \exp(\tau) \operatorname{erfc}(\sqrt{\tau}), \quad (64)$$

which is independent of γ . This integrates to 1, thus the PDF is well-formed for all values of γ (although we are only interested in the case $\gamma \rightarrow \infty$). The mean value of the PDF of ΔT can also be found,

$$\langle \Delta T \rangle = \int_0^\infty d\Delta T \Delta T P_{\Delta T}(\Delta T) = \frac{\tau_d}{2} \int_0^\infty \tau \log\left(\frac{2\tau}{\gamma} + 1\right) P_\tau(\tau) = \frac{\tau_d}{2} \exp\left(-\frac{\gamma}{2}\right) \left[\pi \operatorname{erfi}\left(\sqrt{\frac{\gamma}{2}}\right) - \operatorname{Ei}\left(\frac{\gamma}{2}\right) \right], \quad (65)$$

where $\operatorname{erfi}(x) = -i \operatorname{erf}(ix)$ and $\operatorname{Ei}(x)$ is the exponential integral, see Ref. 39, Ch. 6.2. We note that

$$\lim_{\gamma \rightarrow \infty} \frac{\langle \Delta T \rangle}{\tau_d} \sqrt{\gamma} = \sqrt{\pi/2}, \quad (66)$$

in agreement with the result in Eq. (42) for the threshold $\tilde{\Phi} = 0$.

We can also find that

$$\lim_{\tau \rightarrow \infty} P_\tau(\tau) \tau^{3/2} = \frac{1}{2\sqrt{\pi}}, \quad (67)$$

suggesting that $P_{\Delta T}(\Delta T)$ has an exponential tail for large ΔT .

V. MONTE-CARLO STUDIES

In this section, we will investigate some properties of excess time statistics for which we do not have analytical results. Firstly, we will employ a Monte-Carlo approach for investigating the PDF of ΔT for general γ . Secondly, the question of how quickly excess times converge to their true values will be investigated.

A. PDF of excess times

The PDF of excess times in the case of no pulse overlap was investigated in Sec. IV, and the special case of crossings over the mean value in the case $\gamma \gg 1$ was discussed in Sec. IV B. The search for an expression for the distribution of time until a process crosses a given threshold is not new, and is frequently referred to as the distribution of first passage time. The Laplace transform for the time until a shot noise process crosses a given threshold from below is given by Refs. 46–48. The related problem of the first passage time for an Ornstein-Uhlenbeck process has been investigated by e. g. Refs. 30, 33, and 49.

To the best of the authors knowledge, there is no closed form expression for the distribution of times above threshold, and discussion of numerically computed probability distributions are rare. In this section we therefore present simulation studies of the complementary CDF of ΔT in the case $\lambda = 0$. Determining the PDF of time above threshold by simulating time series of the process as in Fig. 2 and estimating $P_{\Delta T}(\Delta T)$ is prohibitively computationally expensive, particularly for large γ and threshold values. We will therefore use a more direct algorithm.

The algorithm consists of the following steps:

1. At time $t = 0$, a pulse arrives which takes the signal from below to above the threshold L . The signal takes on the value $\Phi(0) > L$ immediately after the pulse arrival. How $\Phi(0)$ is computed is discussed below.
2. This arrival ensures that the signal at least spends a time $t_0 = \tau_d \ln(\Phi(0)/L)$ above the threshold, which is the excess time in the case of no other pulse arrivals in this time interval.
3. Draw a waiting time τ_1 from the exponential waiting time distribution, using the standard numpy Mersenne Twister random number generator. If $\tau_1 > t_0$, the signal decays below the threshold before the next pulse arrives, and the excess time is t_0 . If $\tau_1 < t_0$, the signal now

spends a time

$$t_1 = \tau_d \left[\ln \left(\Phi(0) + A_1 \exp \left(\frac{\tau_1}{\tau_d} \right) \right) - \ln(L) \right] \quad (68)$$

above the threshold, where A_1 is the amplitude associated with the pulse arriving at τ_1 .

4. Draw a new waiting time τ_2 , and compare $\tau_1 + \tau_2$ to t_1 . If $\tau_1 + \tau_2 < t_1$, make t_2 in the same way as above.
5. Continue until the sum of the waiting times would place the arrival of the n 'th pulse after the signal has decayed below the threshold. The time above threshold is then t_{n-1} , and is stored.
6. Repeat as often as necessary, and estimate $P_{\Delta T}(\Delta T)$ from all times above threshold found in steps 1-5 above.

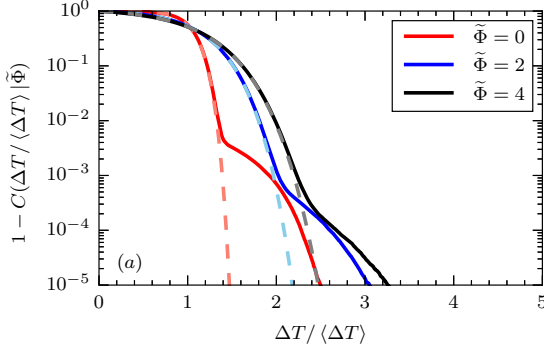
Step 1 requires calculating $\Phi(0)$, which consists of two parts. Assume a stationary filtered Poisson process takes the value $\Phi_- < L$ just before time $t = 0$. A pulse with amplitude A_0 arrives and takes the signal above the threshold, $\Phi(0) = \Phi_- + A_0 > L$. It will be shown in Appendix C that the PDF of $\Phi(0)$ is

$$P_{\Phi(0)}(\Phi(0)) = \frac{1}{\langle A \rangle} \exp \left(-\frac{\Phi(0) - L}{\langle A \rangle} \right), \quad \Phi(0) > L. \quad (69)$$

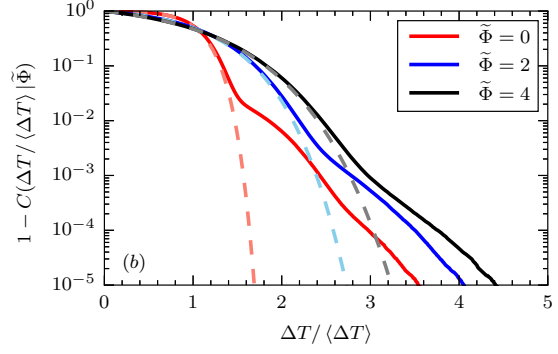
Samples from this distribution are easily drawn using inverse random sampling. The algorithm presented above is reasonably fast, and allows for accurate computation of the empirical CDF.

In Fig. 9, we present plots of $1 - C_{\Delta T/\langle \Delta T \rangle}(\Delta T/\langle \Delta T \rangle)$ as a function of $\Delta T/\langle \Delta T \rangle$ for $\gamma = \{10^{-3}, 10^{-2}, 10^{-1}, 1, 10, 10^2\}$ and various values of the rescaled threshold value $\tilde{\Phi}$. The full lines give the empirical complementary CDF for 10^7 excess time simulations. In Figs. 9a, 9b and 9c, the dashed lines give the analytic complementary CDF for ΔT in the limit $\gamma \rightarrow 0$ given by Eq. (56). This expression matches the simulated results for short times above threshold, but underestimate the result for longer times above threshold. This is due to the fact that for small but finite γ , pulse overlap is significant enough to make longer times above threshold more likely. There is a clear bump in the complementary CDF for $\gamma = 10^{-3}$, which is also visible for $\gamma = 10^{-2}$. This bump signifies the departure of the simulated distribution from the analytic result in the limit $\gamma \rightarrow 0$, and is most likely due to the breakdown of the assumption of no pulse overlap. The bump may signify the arrival of a second pulse after the original pulse.

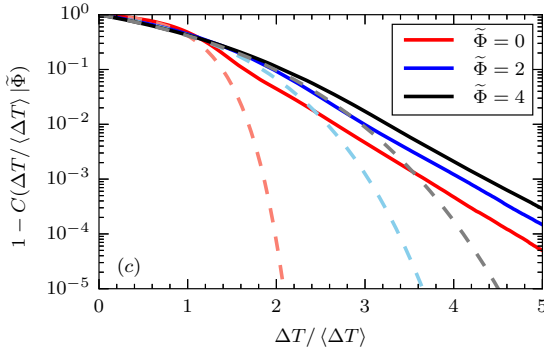
In Figs. 9e and 9f, the dashed line represents the CCDF in the case of $\gamma \gg 1$, from Eq. (63). We have calculated this by calculating $1 - C_\tau(\tau(\Delta T/\langle \Delta T \rangle))$ from Eq. (64), where $\tau(\Delta T/\langle \Delta T \rangle) =$



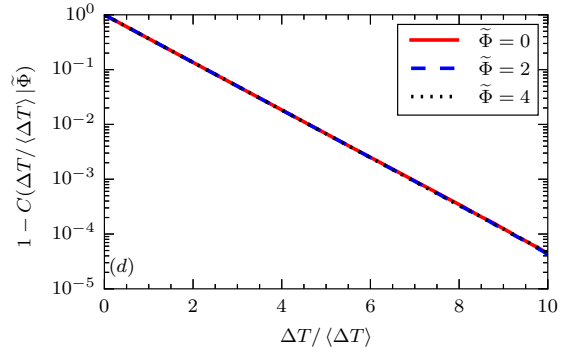
(a) Complementary CDF of time above threshold for $\gamma = 10^{-3}$. Dashed lines show the analytical prediction in the limit $\gamma \rightarrow 0$.



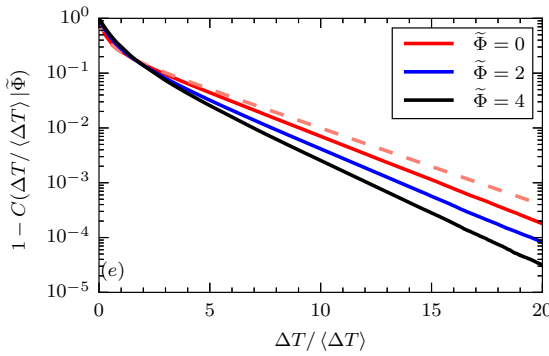
(b) Complementary CDF of time above threshold for $\gamma = 10^{-2}$. Dashed lines show the analytical prediction in the limit $\gamma \rightarrow 0$.



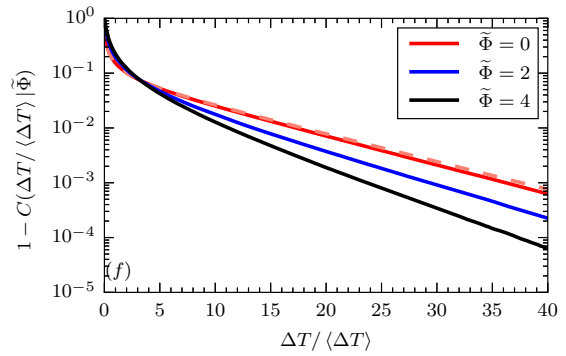
(c) Complementary CDF of time above threshold for $\gamma = 10^{-1}$. Dashed lines show the analytical prediction in the limit $\gamma \rightarrow 0$.



(d) Complementary CDF of time above threshold for $\gamma = 1$.



(e) Complementary CDF of time above threshold for $\gamma = 10$. The dashed line shows analytical prediction for $\tilde{\Phi} = 0$ and $\gamma \gg 1$.



(f) Complementary CDF of time above threshold for $\gamma = 10^2$. The dashed line shows analytical prediction for $\tilde{\Phi} = 0$ and $\gamma \gg 1$.

FIG. 9: Synthetically generated complementary CDF of time above threshold for $\lambda = 0$ and various γ and threshold values.

$\gamma[\exp(2 \langle \Delta T \rangle \Delta T / \tau_d) - 1]/2$ and $\langle \Delta T \rangle$ is found from Eq. (65). The γ -values of the respective figures have been used in this calculation. It is evident that the simulated PDF approaches the analytic PDF for $\gamma \rightarrow \infty$.

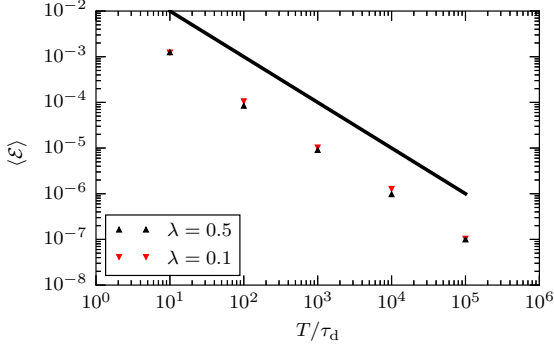
For $\gamma < 1$, the distribution is concave (on the logarithmic scale) and transitions to a convex distribution for $\gamma > 1$. As seen in Fig. 9d, the shape of the distribution for $\gamma = 1$ is an exponential function for all values of the threshold level. Exponential tails for large ΔT are seen for $\gamma = 0.1$ and above. In the case $\gamma \rightarrow \infty$, this was verified analytically, Eq. (67). The exponential tails are not a universal trait of this probability distribution; the Gompertz distribution for ΔT in the case $\gamma \rightarrow 0$ falls off as $\exp(\exp(\Delta T))$.

B. Convergence of excess statistics

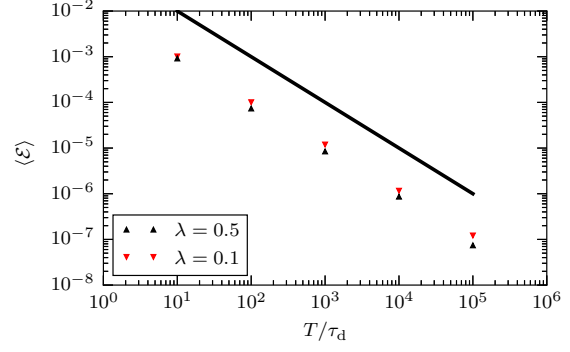
In this section, we will quantify how fast the rate of level crossings converges to the analytical value. The process is as follows:

- Choose a time series length (a number of data points for the time series), γ , λ and Δ_t ; and generate the time series
- Choose 200 threshold values $L_k, k = 0, 1, \dots, 200$ evenly spaced between $\tilde{\Phi} = 2$ and $\tilde{\Phi} = 10$, and estimate the rate of level crossings \hat{X}_k for each L_k .
- Find the value $\mathcal{E} = \frac{1}{200} \sum_{k=1}^{200} \left[\ln(\hat{X}_k) - \ln(X(L_k)) \right]^2$
- Repeat as often as necessary to estimate the mean of \mathcal{E} for different $T, \Delta_t, \gamma, \lambda$.

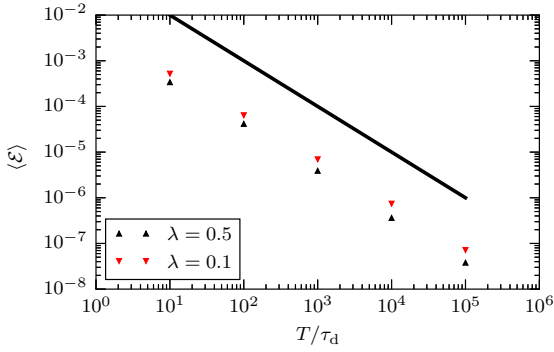
In Fig. 10, we present the estimated mean squared error of synthetic data for $\gamma = \{10^{-1}, 1, 10, 10^2\}$ and $\lambda = \{10^{-1}, 1/2\}$. The algorithm described above was repeated 100 times for each set of parameters. In all cases, the mean squared error decreases with T/τ_d as $(T/\tau_d)^{-1}$. In Figs. 10a-10d, we see that the error for $\lambda = 10^{-1}$ is larger than the error for $\lambda = 1/2$ in all cases. This is most likely a side effect of the algorithm used, where the pulses are forced to arrive at integer multiples of Δ_t . This introduces a slight bias in the synthetic data, which is lower for more symmetric pulses. It is also evident from Figs. 10e and 10f that the error decreases with increasing γ . Higher γ for equal T/τ_d signifies more pulses, which converges more quickly to the stationary distribution.



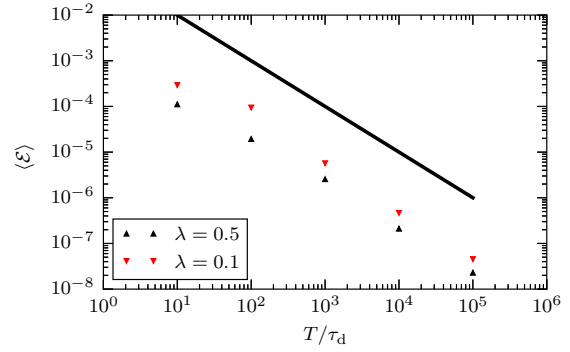
(a) Mean squared error of synthetic data for $\gamma = 10^{-1}$ and various λ .



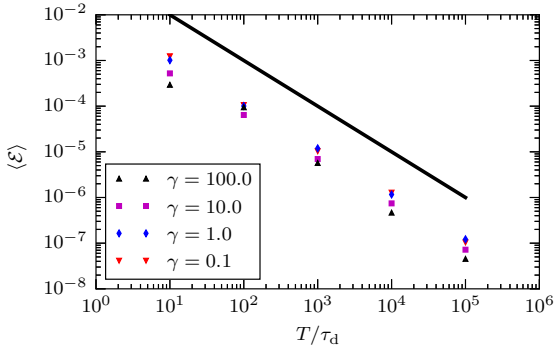
(b) Mean squared error of synthetic data for $\gamma = 1$ and various λ .



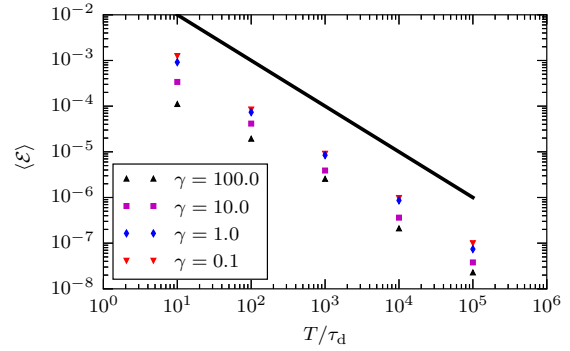
(c) Mean squared error of synthetic data for $\gamma = 10$ and various λ .



(d) Mean squared error of synthetic data for $\gamma = 10^2$ and various λ .



(e) Mean squared error of synthetic data for $\lambda = 10^{-1}$ and various γ .



(f) Mean squared error of synthetic data for $\lambda = 1/2$ and various γ .

FIG. 10: Mean squared error of synthetic data for various γ and λ . In all cases, the solid black line gives τ_d/T .

VI. CONCLUSION

In conclusion, a previously suggested stochastic model for intermittent fluctuations in the scrape-off layer of magnetically confined plasmas has been considered. The model consists of a super-position of pulses with a fixed, exponential pulse shape and exponentially distributed amplitudes arriving according to a Poisson process. This process has shown itself to provide a good description of experimental data from the scrape-off layer.^{4,6–10,16} In this contribution, the derivative of this process was discussed, and the joint probability density function of the random variable and its derivative was derived. The joint PDF was used to obtain predictions for level crossings and average excess times for fluctuations above a given threshold. These predictions depend on two model parameters, the intermittency parameter γ and the pulse shape asymmetry parameter λ . It is shown that the functional shape of the rate of level crossings with the threshold level is strongly dependent on the intermittency parameter γ of the process, while the functional shape of the average excess time varies little with the parameter γ , suggesting that the rate of level crossings might be a more useful tool in comparing the model to experimental data in order to assess intermittency effects. The rate of level crossings has compared favorably to large-amplitude fluctuations in SOL plasmas.⁹ In both cases, the functional shape does not depend on λ , although the absolute value of the rate of level crossings and average time above threshold depends on λ . The limit of $\lambda \rightarrow 0$ was considered, and was shown to be in agreement with previous works using different methods.^{32,34} The limits of highly intermittent signals as well as the normal limit were investigated. The normal limit was shown to be in agreement with the well-known Rice's formula,²² and was shown to have qualitatively different behaviour for $\lambda = 0, 1$ and $\lambda \in (0, 1)$. The rate of level crossings for a model with Laplace distributed pulse amplitudes was also considered and compared to the model with exponentially distributed amplitudes. This model has been compared to the distribution of radial velocity in SOL plasmas.^{6?}

The probability density function of the time the stochastic process spends above the threshold was found analytically in both the limit of strong intermittency for general threshold level and in the normal limit for threshold equal to the mean value, adapted from studies of Ornstein-Uhlenbeck-processes.^{30,33} By a Monte-Carlo study of synthetically generated times above threshold, both limits were shown to hold, and the shape of the PDF of time above threshold was presented. Monte-Carlo studies were also done to confirm the convergence of the rate of level crossings to the analytical expression.

Considering comparisons to experimental data, the results presented here provide two major improvements over the classical Rice's formula in the case of intermittent fluctuations. Firstly, any discrepancy between the normal limit for excess time statistics and measurement data has previously been interpreted as a signature of intermittency in the process. The formulas derived here quantifies the level of intermittency by the model parameters λ and γ . Secondly, Rice's formula requires the rms-value of the derivative of the signal, which is difficult if not impossible to reliably estimate for discretely sampled data. While $\dot{\Phi}_{\text{rms}}/\Phi_{\text{rms}}$ in Eqs. (4) and 6 can be considered a free fit parameter, it is unclear what the meaning of this parameter is. In contrast, estimates for λ and γ can be found from the signal using the lowest order moments of Φ and its correlation function or frequency power spectrum.^{6,7}

Even though the total time above a given threshold level may be the same for realizations of two different intermittent processes, this can be realized through either many short plasma bursts or few but long lasting bursts events. This may have profound implications for plasma-wall interactions in magnetically confined plasmas, since long lasting, large amplitude events can lead to severe damaging while the system can recover from the damaging impacts of shorter burst events depending on their frequency of occurrence.^{24,25} Thus accurately predicting the rate of level crossings and average excess times for an intermittent process is of considerable interest to statistical modelling of fluctuations in the boundary region of magnetically confined plasmas. In future work, the novel predictions presented here will be further compared to experimental measurement data from the scrape-off layer of magnetically confined plasmas.

ACKNOWLEDGEMENTS

This work was supported with financial subvention from the Research Council of Norway under grant 240510/F20.

Appendix A: The joint PDF of Φ and Θ in the normal limit

We will investigate the joint PDF of Φ and Θ given by Eq. (30) in the limit $\gamma \rightarrow \infty$. We begin by changing variables to the normalized

$$\tilde{\Phi} = \frac{\Phi - \langle \Phi \rangle}{\Phi_{\text{rms}}}, \quad (\text{A1})$$

$$\tilde{\Theta} = \frac{\Theta}{\Theta_{\text{rms}}}. \quad (\text{A2})$$

where the moments of Φ and Θ are given in Eqs. (18) and (22) respectively. Then we have

$$\begin{aligned} P_{\tilde{\Phi}\tilde{\Theta}}(\tilde{\Phi}, \tilde{\Theta}) &= \Phi_{\text{rms}} \Theta_{\text{rms}} P_{\Phi\Theta}(\Phi_{\text{rms}}\tilde{\Phi} + \langle \Phi \rangle, \Theta_{\text{rms}}\tilde{\Theta}) \\ &= \frac{(\gamma\lambda)^{\gamma\lambda-1/2} \exp(-\gamma\lambda) [\gamma(1-\lambda)]^{\gamma(1-\lambda)-1/2} \exp(-\gamma(1-\lambda))}{\Gamma(\gamma\lambda) \Gamma(\gamma(1-\lambda))} \exp(-\sqrt{\gamma}\tilde{\Phi}) \\ &\quad \times \left[\frac{\tilde{\Phi}}{\sqrt{\gamma}} + \sqrt{\frac{1-\lambda}{\lambda}} \frac{\tilde{\Theta}}{\sqrt{\gamma}} + 1 \right]^{\gamma\lambda-1} \left[\frac{\tilde{\Phi}}{\sqrt{\gamma}} - \sqrt{\frac{\lambda}{1-\lambda}} \frac{\tilde{\Theta}}{\sqrt{\gamma}} + 1 \right]^{\gamma(1-\lambda)-1}. \end{aligned} \quad (\text{A3})$$

By Stirling's formula, both first fractions are equal to $1/\sqrt{2\pi}$. Using the notation

$$\alpha = \tilde{\Phi} + \sqrt{\frac{1-\lambda}{\lambda}} \tilde{\Theta}, \quad (\text{A4})$$

$$\beta = \tilde{\Phi} - \sqrt{\frac{\lambda}{1-\lambda}} \tilde{\Theta}, \quad (\text{A5})$$

we have that $\tilde{\Phi} = \lambda\alpha + (1-\lambda)\beta$ and

$$\begin{aligned} \lim_{\gamma \rightarrow \infty} P_{\tilde{\Phi}\tilde{\Theta}}(\tilde{\Phi}, \tilde{\Theta}) &= \lim_{\gamma \rightarrow \infty} \frac{1}{2\pi} \exp(\sqrt{\gamma}[\lambda\alpha + (1-\lambda)\beta]) \left(\frac{\alpha}{\sqrt{\gamma}} + 1 \right)^{\gamma\lambda-1} \left(\frac{\beta}{\sqrt{\gamma}} + 1 \right)^{\gamma(1-\lambda)-1} \\ &= \frac{1}{2\pi} \exp \left(\lim_{\gamma \rightarrow \infty} \sqrt{\gamma}[\lambda\alpha + (1-\lambda)\beta] \right. \\ &\quad \left. + (\gamma\lambda - 1) \log \left(\frac{\alpha}{\sqrt{\gamma}} + 1 \right) + [\gamma(1-\lambda) - 1] \log \left(\frac{\beta}{\sqrt{\gamma}} + 1 \right) \right) \\ &= \frac{1}{2\pi} \exp \left(\lim_{\gamma \rightarrow \infty} \sqrt{\gamma}[\lambda\alpha + (1-\lambda)\beta] + (\gamma\lambda - 1) \left[\frac{\alpha}{\sqrt{\gamma}} - \frac{1}{2} \left(\frac{\alpha^2}{\sqrt{\gamma}} \right)^2 + \mathcal{O}(\gamma^{-3/2}) \right] \right. \\ &\quad \left. + [\gamma(1-\lambda) - 1] \left[\frac{\beta}{\sqrt{\gamma}} - \frac{1}{2} \left(\frac{\beta^2}{\sqrt{\gamma}} \right)^2 + \mathcal{O}(\gamma^{-3/2}) \right] \right) \\ &= \frac{1}{2\pi} \exp \left(\lim_{\gamma \rightarrow \infty} -\frac{\lambda}{2} \alpha^2 - \frac{1-\lambda}{2} \beta^2 + \mathcal{O}(\gamma^{-1/2}) \right) \\ &= \frac{1}{2\pi} \exp \left(-\frac{\tilde{\Phi}^2 + \tilde{\Theta}^2}{2} \right). \end{aligned} \quad (\text{A6})$$

And in the limit of $\gamma \rightarrow \infty$, the joint PDF of $\tilde{\Phi}$ and $\tilde{\Theta}$ approaches a joint normal distribution of independent variables.

Appendix B: Upper incomplete Gamma function to error function

The regularized upper incomplete Gamma function is defined in Ref. 39, Ch. 8.2. We have

$$\lim_{\gamma \rightarrow \infty} Q(\gamma, \sqrt{\gamma}\tilde{\Phi} + \gamma) = \lim_{\gamma \rightarrow \infty} \frac{1}{\Gamma(\gamma)} \int_{\sqrt{\gamma}\tilde{\Phi} + \gamma}^{\infty} dt t^{\gamma-1} \exp(-t). \quad (\text{B1})$$

By substituting $u = (t - \gamma)/\sqrt{\gamma}$ and using that $\gamma\Gamma(\gamma) = \Gamma(\gamma + 1)$, this expression becomes

$$\lim_{\gamma \rightarrow \infty} \frac{\gamma^{3/2}}{\Gamma(\gamma + 1)} \int_{\tilde{\Phi}}^{\infty} du (\sqrt{\gamma}u + \gamma)^{\gamma-1} \exp(-\sqrt{\gamma}u - \gamma) = \int_{\tilde{\Phi}}^{\infty} du \lim_{\gamma \rightarrow \infty} \frac{\gamma^{\gamma+1/2} \exp(-\gamma)}{\Gamma(\gamma + 1)} \left(\frac{u}{\sqrt{\gamma}} + 1 \right)^{\gamma-1} \exp(-\sqrt{\gamma}u). \quad (\text{B2})$$

The fraction is $1/\sqrt{2\pi}$ by Stirling's formula, and using Eq. (A6) with $\beta = 0$, $\lambda = 1$, we have that

$$\lim_{\gamma \rightarrow \infty} Q(\gamma, \sqrt{\gamma}\tilde{\Phi} + \gamma) = \frac{1}{\sqrt{2\pi}} \int_{\tilde{\Phi}}^{\infty} du \exp\left(-\frac{u^2}{2}\right) = \frac{1}{2} \operatorname{erfc}\left(\frac{\tilde{\Phi}}{\sqrt{2}}\right). \quad (\text{B3})$$

Appendix C: The truncated exponential distribution

Consider a stationary stochastic process Φ consisting of random pulses. Assume the pulses have a positive jump at the arrival time, and only are non-zero after the arrival time. Just before $t = 0$ it is below the threshold L ;

$$\Phi_- = \lim_{\epsilon \rightarrow 0} \Phi(-\epsilon) \quad (\text{C1})$$

with $\Phi_- < L$. A pulse with amplitude A arrives at $t = 0$, taking the signal above the threshold:

$$\Phi_- + A = \Phi_0 > L. \quad (\text{C2})$$

It is assumed that A is exponentially distributed with mean value $\langle A \rangle$. Φ_- can in principle have an arbitrary distribution. The distribution of Φ_0 is then found from:

$$P_{\Phi_0}(\Phi_0) = \frac{\partial}{\partial \Phi_0} C_{\Phi_0}(\Phi_0) = \frac{\partial}{\partial \Phi_0} \iint_{\Phi_- + A < \Phi_0} dA d\Phi_- P_{\Phi_-}(\Phi_- | \Phi_- < L) P_A(A | A + \Phi_- > L), \quad (\text{C3})$$

where

$$P_{\Phi_-}(\Phi_- | \Phi_- < L) = \frac{P_{\Phi_-}(\Phi_-)}{C_{\Phi_-}(L)}, \quad \Phi_- < L \quad (\text{C4})$$

and

$$P_A(A | A + \Phi_- > L) = \frac{P_A(A)}{1 - C_A(L - A)}, \quad A > L - \Phi_-. \quad (\text{C5})$$

The truncated distributions are calculated by using the method given in Ref. 43. This gives

$$P_{\Phi_0}(\Phi_0|L) = \frac{\partial}{\partial \Phi_0} \int_0^L d\Phi_- \frac{P_{\Phi_-}(\Phi_-)}{C_{\Phi_-}(L)[1 - C_A(L - \Phi_-)]} \int_{L-\Phi_-}^{\Phi_0-\Phi_-} dA P_A(A). \quad (C6)$$

The derivative with respect to Φ_0 can be brought inside the first integral, and we have that

$$\frac{\partial}{\partial \Phi_0} \frac{1}{1 - C_A(L - \Phi_-)} \int_{L-\Phi_-}^{\Phi_0-\Phi_-} dA P_A(A) = P_A(\Phi_0 - L), \quad \Phi_0 > L, \quad (C7)$$

where we have used that A is exponentially distributed. This does not depend on Φ_- , so we have

$$P_{\Phi_0}(\Phi_0|L) = P_A(\Phi_0 - L) \frac{\int_0^L d\Phi_- P_{\Phi_-}(\Phi_-)}{C_{\Phi_-}(L)}, \quad \Phi_0 > L. \quad (C8)$$

which simplifies to

$$P_{\Phi_0}(\Phi_0|L) = \frac{1}{\langle A \rangle} \exp\left(-\frac{\Phi_0 - L}{\langle A \rangle}\right), \quad \Phi_0 > L. \quad (C9)$$

Thus, if we assume exponentially distributed pulse amplitudes and pulses with jumps as described above, the distribution of the stationary Φ plays no role in the distribution of the jump above the threshold. In particular, for a shot noise process with $\lambda \rightarrow 0$ and $\gamma \rightarrow \infty$, the process is normally distributed, but the value of the signal just after the threshold is crossed is exponentially distributed.

REFERENCES

- ¹R. A. Pitts, J. P. Coad, D. P. Coster, G. Federici, W. Fundamenski, J. Horacek, K. Krieger, A. Kukushkin, J. Likonon, G. F. Matthews, M. Rubel, J. D. Strachan, and J.-E. Contributors, Plasma Phys. Control. Fusion **47**, B303 (2005).
- ²B. Lipschultz, X. Bonnin, G. Counsell, A. Kallenbach, A. Kukushkin, K. Krieger, A. Leonard, A. Loarte, R. Neu, R. Pitts, T. Rognlien, J. Roth, C. Skinner, J. Terry, E. Tsitrone, D. Whyte, S. Zweben, N. Asakura, D. Coster, R. Doerner, R. Dux, G. Federici, M. Fenstermacher, W. Fundamenski, P. Ghendrih, A. Herrmann, J. Hu, S. Krasheninnikov, G. Kirnev, A. Kreter, V. Kurnaev, B. LaBombard, S. Lisgo, T. Nakano, N. Ohno, H. Pacher, J. Paley, Y. Pan, G. Pautasso, V. Philipps, V. Rohde, D. Rudakov, P. Stangeby, S. Takamura, T. Tanabe, Y. Yang, and S. Zhu, Nucl. Fusion **47**, 1189 (2007).
- ³D. A. D'Ippolito, J. R. Myra, and S. J. Zweben, Phys. Plasmas **18**, 060501 (2011).
- ⁴O. E. Garcia, S. M. Fritzner, R. Kube, I. Cziegler, B. LaBombard, and J. L. Terry, Phys. Plasmas **20**, 055901 (2013).

- ⁵O. E. Garcia, J. Horacek, and R. A. Pitts, Nucl. Fusion **55**, 062002 (2015).
- ⁶A. Theodorsen, O. E. Garcia, J. Horacek, R. Kube, and R. A. Pitts, Plasma Phys. Control. Fusion **58**, 044006 (2016), arXiv:1604.08163.
- ⁷R. Kube, A. Theodorsen, O. E. Garcia, B. LaBombard, and J. L. Terry, Plasma Phys. Control. Fusion **58**, 054001 (2016).
- ⁸O. Garcia, R. Kube, A. Theodorsen, J.-G. Bak, S.-H. Hong, H.-S. Kim, t. K. P. Team, and R. Pitts, Nucl. Mater. Energy (2016), 10.1016/j.nme.2016.11.008.
- ⁹A. Theodorsen, O. Garcia, R. Kube, B. LaBombard, and J. Terry, Nucl. Fusion.
- ¹⁰R. Kube, O. Garcia, A. Theodorsen, D. Brunner, B. LaBombard, and J. Terry, .
- ¹¹S. O. Rice, “Mathematical Analysis of Random Noise,” (1944).
- ¹²O. E. Garcia, Phys. Rev. Lett. **108**, 265001 (2012).
- ¹³O. E. Garcia, R. Kube, A. Theodorsen, and H. L. Pécseli, Phys. Plasmas **23**, 052308 (2016).
- ¹⁴R. Kube and O. E. Garcia, Phys. Plasmas **22**, 012502 (2015).
- ¹⁵A. Theodorsen and O. E. Garcia, Phys. Plasmas **23**, 040702 (2016).
- ¹⁶F. Sattin, M. Agostini, P. Scarin, N. Vianello, R. Cavazzana, L. Marrelli, G. Serianni, S. J. Zweben, R. J. Maqueda, Y. Yagi, H. Sakakita, H. Koguchi, S. Kiyama, Y. Hirano, and J. L. Terry, Plasma Phys. Control. Fusion **51**, 055013 (2009).
- ¹⁷A. S. Bergsaker, Å. Fredriksen, H. L. Pécseli, and J. K. Trulsen, Phys. Scr. **90**, 108005 (2015).
- ¹⁸A. Theodorsen, O. E. Garcia, and M. Rypdal, Phys. Scr..
- ¹⁹H. Pécseli, *Fluctuations in physical systems* (Cambridge University Press, 2000) p. 200.
- ²⁰O. E. Garcia and A. Theodorsen, Phys. Plasmas **24**, 020704 (2017).
- ²¹O. Garcia and A. Theodorsen, Phys. Plasmas.
- ²²S. O. Rice, Bell Syst. Tech. J. **24**, 46 (1945).
- ²³L. Kristensen, M. Casanova, M. S. Courtney, and I. Troen, Boundary-Layer Meteorol. **55**, 91 (1991).
- ²⁴H. Sato, H. L. Pécseli, and J. Trulsen, J. Geophys. Res. **117**, A03329 (2012).
- ²⁵L. Fattorini, Å. Fredriksen, H. L. Pécseli, C. Riccardi, and J. K. Trulsen, Plasma Phys. Control. Fusion **54**, 085017 (2012).
- ²⁶F. Dalmao and E. Mordecki, Extremes **18**, 15 (2015).
- ²⁷I. Bar-David and A. Nemirovsky, IEEE Trans. Inf. Theory **IT-18**, 8 (1972).
- ²⁸R. Barakat, J. Opt. Soc. Am. A **5**, 1244 (1988).
- ²⁹M. Leadbetter and G. Spaniolo, Aust. New Zeal. J. Stat. **46**, 173 (2004).

- ³⁰L. Alili, P. Patie, and J. L. Pedersen, *Stoch. Model.* **21**, 967 (2005).
- ³¹K. I. Hopcraft, P. C. Ingre, and E. Jakeman, *Phys. Rev. E* **76**, 031134 (2007).
- ³²E. Daly and A. Porporato, *Phys. Rev. E* **81**, 061133 (2010).
- ³³C. Yi, *Quant. Financ.* **10**, 957 (2010).
- ³⁴H. Biermé and A. Desolneux, *J. Appl. Probab.* **49**, 100 (2012).
- ³⁵N. Campbell, *Proc. Camb. Philol. Soc.* **15**, 117 (1909).
- ³⁶E. Parzen, *Stochastic Processes* (Society for Industrial and Applied Mathematics, 1999).
- ³⁷S. B. Lowen and M. C. Teich, *Fractal-Based Point Processes*, Wiley Series in Probability and Statistics (John Wiley & Sons, Inc., Hoboken, NJ, USA, 2005).
- ³⁸L. Bondesson, *Adv. Appl. Probab.* **14**, 855 (1982).
- ³⁹F. W. J. Olver, A. B. Olde Daalhuis, D. W. Lozier, B. I. Schneider, R. F. Boisvert, C. W. Clark, B. R. Miller, and B. V. Saunders, “NIST Digital Library of Mathematical Functions,” <http://dlmf.nist.gov/>, Release 1.0.14 of 2016-12-21.
- ⁴⁰This is a correction to ϑ given in Ref. 15. This leads to corrections in the rms-value of Θ and the joint PDF between Φ and Θ , but not the excess statistics.
- ⁴¹T. J. Kozubowski and K. Podgórski, *Comput. Stat.* **15**, 531 (2000).
- ⁴²W. J. Reed, in *Adv. Distrib. Theory, Order Stat. Inference* (Birkhäuser Boston, Boston, MA, 2006) pp. 61–74.
- ⁴³J. W. Stark, H.: Woods, *Probability, Statistics and Random Processes for Engineers*, 4th ed. (Pearson Education, 2012).
- ⁴⁴D. J. Olive, “Some Useful Distributions,” in *Stat. Theory Inference* (Springer International Publishing, Cham, 2014) pp. 291–357.
- ⁴⁵C. E. Rasmussen, “Gaussian Processes in Machine Learning,” in *Adv. Lect. Mach. Learn. ML Summer Sch. 2003, Canberra, Aust. Febr. 2 - 14, 2003, Tübingen, Ger. August 4* edited by O. Bousquet, U. von Luxburg, and G. Rätsch (Springer Berlin Heidelberg, Berlin, Heidelberg, 2004) pp. 63–71.
- ⁴⁶A. Tsurui and S. Osaki, *Stoch. Process. their Appl.* **4**, 79 (1976).
- ⁴⁷D. Perry, W. Stadje, and S. Zacks, *Stoch. Model.* **17**, 25 (2001).
- ⁴⁸A. Novikov, R. Melchers, E. Shinjikashvili, and N. Kordzakhia, *Probabilistic Eng. Mech.* **20**, 57 (2005).
- ⁴⁹Y. Madec and C. Japhet, *Math. Biosci.* **189**, 131 (2004).